UNIVERSITAT POLITÈCNICA DE CATALUNYA

# MASTER THESIS

# Study and implementation of the stability and control system of a mini-launcher

Ruizhi Yuan

**SUPERVISED BY**

Jordi Gutiérrez
Joshua Tristancho

**Universitat Politècnica de Catalunya**
**Master in Aerospace Science & Technology**
July 2011

# Study and implementation of the stability and control system of a mini-launcher

BY

Ruizhi Yuan

DIPLOMA THESIS FOR DEGREE

Master in Aerospace Science and Technology

AT

Universitat Politècnica de Catalunya

SUPERVISED BY:

Jordi Gutiérrez

Joshua Tristancho

Applied Physics department

# ABSTRACT

In this Master Thesis Work (TFM), the proposal is to study some aspects of the stability, like flutter effects, over a small space launcher (less than 100 kg including propellant and payload). This mini-launcher is called Wiki-Launcher and it is part of a space mission done by the Wikisat team. This team is participating in the N-Prize competition that consists of designing a femto-satellite (Less than 20 grams) and injecting it into orbit by a home-made launcher that costs less than 1,000 Pounds Sterline before September, 2012.

Flutter is a kind of self-excited aeroelastic unstable phenomenon where the safety of the flight vehicles may be threatened. Flutter can be catastrophic once it occurs and must be avoided. Thus it is mandatory to verify the flutter boundary of the flight launcher by performing wind-tunnel and flight tests, which always consume plenty of time and money. Efficient and effective flutter prediction methods are in demand so as to accelerate the process of tests, as well as ensuring the safety during the tests.

The flutter boundary of a mini-launcher is predicted using the data-based parameter-varying model. The core algorithms are the well-developed linear fraction transform (LFT) and $\mu$-analysis. Compared with the former model-based $\mu$ method, this approach requires less model information and is easier to handle.

In this thesis, we try to check if this method is able to be implemented in a low cost way for the Wiki-Launcher that could be extended to other larger launchers.

**Keywords:** Flutter prediction, Mini-launcher, Data-based parameter-varying model, Wind tunnel

# Acknowledgements

I'm grateful to my parents and my friends for their constant support and inspiration to me during this work.

Particular thanks are expressed to Joshua Tristancho and Jordi Gutiérrez for giving me the opportunity to participate in this project and the WikiSat team, and especially Joshua Tristancho for his continuous help and support during this research work.

Grateful thanks are due to all the other WikiSat members who helped and supported me with the realization of the thesis, specially Victor Kravchenco, Roberto Rodríguez, Esteve Bardolet, Juan Martínez, Javier Pérez, Sonia Pérez, Lara Navarro and Raquel González, etc.

And my deep appreciation also goes to Beihang University and my tutors there, Professor Yang and Wu, for their consistent support to me.

Acknowledgment is made to the EETAC school for the facilities and tools they have provided to support this work.

Also I want to thank our partners from Team FREDNET and D47 for their support to our group in general, and some parts of my work in particular.

# CONTENTS

# LIST OF FIGURES

# LIST OF TABLES

# INTRODUCTION

In engineering terms, flutter means a vibration that can amplify into structural damage. It is a kind of self-excited aeroelastic unstable phenomenon, due to the interaction among inertial, elastic and aerodynamic forces. The safety of the flight vehicles may be threatened by flutter, which often causes catastrophic failures once it occurs. Thus it is essential to verify that the flight vehicles are free from flutter by performing wind-tunnel and flight tests, which always consumes plenty of time and money. Efficient and effective flutter prediction methods are in demand so as to accelerate the process of tests, as well as ensuring the safety during the tests.

There are many traditional data-based methods to predict the onset of flutter during flight testing[1], such as Modal Damping Extrapolation[2], Envelope Function and Flutter Margin (Zimmerman-Weissenburger method)[3], etc. The advantage of the data-based methods are that they require little model information and are easy to handle, but the shortcomings are also obvious. Due to the rather noisy test data and various flutter mechanics, a simple to extrapolating the indicating parameters extracted from test data for the critical flutter point may be biased. Then a model-based $\mu$ method approach combining system model and flight data is utilized, for instance the flutterometer[4]. With the initial finite element and aerodynamics as the nominal model unchanged, only the uncertainty operators of the robust aeroelastic model are updated using the test data. The flutter bounds depend on the estimation and validation of the uncertainty. Match-point solutions are derived for robust flutter analysis[5]. Recently a Parameter-Varying Estimation (PVE) framework for Robust flutter prediction[6] is proposed to certify an aircraft during envelope expansion. The core algorithms are the well-developed linear fraction transform (LFT) and $\mu$-analysis[7]. This new approach, built upon an integrated parameter-estimation methods, can only based on the test data, given a chance to be easily extended to predict the onset of limit-cycle oscillations (LCO)[8]. The details of the procedure for this data-based prediction approach are given in Chapter 2.

This data-based prediction approach has proved to be effective and feasible in real flight testing of ATW wing[6]. But the application to mini-launcher may be a different scenario. There are several special features for a mini-launcher, which may bring a new challenge for the flutter prediction. The size and mass of sensors are comparable to the size and mass of a model of the launcher and they can modify the results from the model to the real launcher. Models are not allowed, it is necessary to work with the real one. To avoid interferences, the only way to do not disturb the results is to use the build-in sensors; using so the same ones from experiments to real cases. The fact that sizes are less than one meter, frequency range to study is also different for traditional aircraft flutter studies. The symmetry of the launcher allow us to use a simplified studies where we only need to study one axis that is repeated very often in any radial direction. There are no cantilever structures, there are mono-coke structures instead. This kind of flutter are also different from a traditional wing in an aircraft. Another important difference from atmospheric flight is the absence of atmosphere where the flutter is coming not form the outside flow but from the combustion chamber flow. Then the aerodynamic study is only inside the combustion chamber and nozzle, and not for the whole launcher. Modification may be needed to improve the prediction methods like ranges, intervals or sensor positioning. Then the

wind-tunnel tests are designed to implement the prediction approach. Finally, a real flight test is performed to verify the prediction results.

In this master thesis, the flutter boundary of a mini-launcher is tried to be predicted through the data-based parameter-varying model. The well-developed linear fraction transform (LFT) and $\mu$-analysis are the core algorithm used. Compared with the former model-based $\mu$ method, this approach requires less real model information[4], besides it is easier to handle and takes less time and effort.

The launcher in study is the so-called WikiLauncher that is the mini-launcher category in less than $100$ kilograms of wet mass and able to put a swarm of femto-satellites. Femto-satellites have a mass less than $100$ grams. Some authors like Barnhart in [9] have proposed the use of really light satellites and others like Jove in [10] have proposed the use of reduced sized launchers. The WikiLauncher is designed to inject femto-satellites in a Low Earth Orbit (LEO). Mainly we focused on the second stage because it is the most demanding situation that this kind of structures should suffer.

We are very interested in the aerodynamic effects in the vacuum and how the inner flow and non-external aerodynamics affect under a certain boundary, provoking a flutter condition. For this reason, firstly it is necessary to know well the behavior of the launcher without and with inner flow in order to see what are the vibration modes. These modes are only produced by the mass distribution and not by the aerodynamic loads around it, something that is different from atmospheric flights. Subsonic wind tunnels tests are used for the initial flutter estimation as a part of the qualification campaign. Real flights are also required to verify the accuracy of the method which is a data-based $\mu$ approach for flutter prediction.

In summary, the outline of this thesis is as follows. In Chapter 1, foundational knowledge about aeroelasticity study area and specially an unstable phenomenon flutter are introduced. Then the features of a mini-launcher, which are the most interesting investigation object within this thesis, are illustrated. Finally, the challenge of flutter prediction for this kind of unique Wiki-Launcher is discussed, and parameter-varying estimation (PVE) approach is proposed to solve this problem.

The PVE approach is further explained in Chapter 2, and the implementation of the method is concluded into a procedure of three steps in a concise way. The Chapter 3 gives two typical application cases for the proposed PVE method. One is a simulated prototypical pitch and plunge aeroelastic system, and the other is from a real scaled half-model airplane wind tunnel test, which have validated the effectiveness of PVE method. Then the PVE approach is tried to be tested for the application to mini-launcher through both wind tunnel test and ground launch test, which are respectively described in Chapter 4 and Chapter 5.

# CHAPTER 1. AEROELASTIC STABILITY OF A MINI-LAUNCHER

In this Chapter, a brief introduction to dynamic aeroelasticity is given, including its interdisciplinary nature, related accidents in history, and some design concerns for high-performance flight vehicles. Then it focuses on the investigation of a mini-launcher, called Wiki-Launcher, which is a rather new area. The possible challenges for flutter analysis of the mini-launcher are discussed. Finally, a recently developed data-based parameter-varying model extracted from test data is proposed to meet the challenge.

## 1.1. Dynamic Aeroelasticity - Flutter

Aeroelasticity is a field of study concerned with the interaction between the deformation of an elastic structure in the airstream and the resulting aerodynamic forces.[15] As a typical interdisciplinary area, it may involve aerodynamics, elasticity and dynamics. With modern servo control systems and more flexible structures, a study of aeroelastic effects with the interaction of control system, called aeroservoelasticity, is developing recently. A schematic interpretation among all these disciplines is shown on figure 1.1.

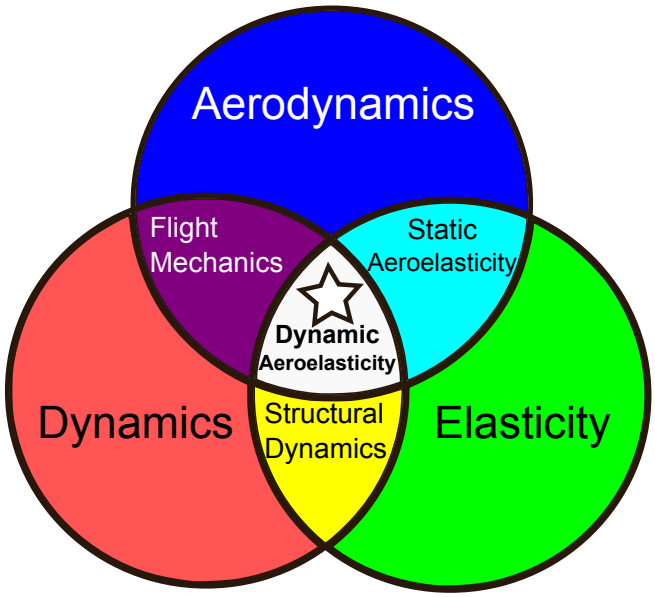


Figure 1.1: Nature of Aeroelasticity - Interdisciplinary Coupling

As depicted by figure 1.1, aeroelasticity usually can be classified into two categories, static and dynamic aeroelasticity. Aeroelastic dynamic response of flight vehicles is a combined result of inertial and elastic structural forces, aerodynamic forces induced by the static or dynamic deformation of the structure, and external disturbance forces. The equation of motion of the aeroelastic system [16] can be written in time domain:

$$\bar{\mathbf{M}}\ddot{\mathbf{x}}(t)+\bar{\mathbf{C}}\dot{\mathbf{x}}(t)+\bar{\mathbf{K}}\mathbf{x}(t)=\mathbf{F}(t) \tag{1.1}$$

where $\bar{\mathbf{M}}$, $\bar{\mathbf{C}}$, $\bar{\mathbf{K}}$ are the generalized mass, damping and stiffness matrices; $\mathbf{x}(t)$ is the structural deformation.

In the center part that means an intercross of the three circles, lies the dynamic aeroelasticity, considering the interaction among inertial, elastic and aerodynamic forces. Dynamic aeroelastic problems are always of greater concern since either immediate disaster or long-term fatigue may happen. Flutter is a rather typical kind of dynamic aeroelastic phenomenon. As a self-excited oscillator, the vibration of the structure absorbs energy from the airstream and the amplitude of the periodic motion tends to increase so rapidly that the structure may be destroyed in a few seconds. That's why flutter is always considered to be a dangerous threaten to the safety of flight vehicles.

The first recorded flutter incident happened in 1916. The Handley Page O/400 bomber experienced violent tail oscillation due to lack of torsional rigidity. Aircraft accidents attributed to flutter becomes a major design concern during First World War and remains so today.[2]

Design concern with flutter is of significant importance to aerospace as well. As the world's first supersonic weapon, the infamous V-2 rocket had no wings to flutter, only tail-fin stabilizers. Surprisingly, because of flutter, about 70 early V-2 crashed or veered off course as the rocket arrived at supersonic speed. It brought a major obstacle that confronted the German designers. In this case, many lives were saved and the world's outcome may be altered due to flutter problem!

The V-2 is where panel flutter was discovered. The rocket structure was a thin container, and it was too flexible to sustain the forces encountered in transonic flight. As V-2 increased from subsonic to supersonic speed, its metal skin shook apart.

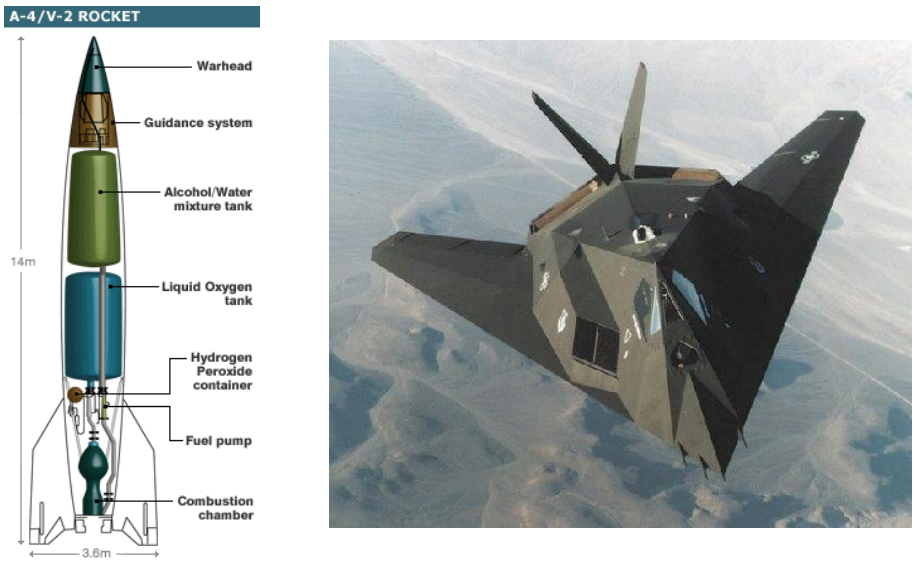


Figure 1.2: V-2 Rocket (Left), F-117 Nighthawk Stealth Aircraft (Right) [1]

Flutter still challenges designers of high-performance flight vehicles. As recently as September 1997, wing flutter caused an F-117A Nighthawk to lose most of one wing and crash at an air show. Flutter can be catastrophic and must be avoided.

[1] (left) http://v2rocket.com, (right) http://xidong.net

The developing procedure to ensure the flight vehicles to be free from flutter consist of flutter theoretical calculation, scaled wind tunnel model test, ground vibration test and flight flutter test, etc. There are several engineering solutions techniques for classical flutter, for instance the $k$ Method or the $p-k$ Method.[15]

Flight tests are the final and critical step to demonstrate that the vehicles are flutter free, and they are partially based on the calculation and ground test results. By using the real model to flight under real conditions, more accurate stable properties can be obtained. But on the other hand, the flight tests are of rather high risk and expense, as well as time-consuming. A typical flutter test procedure is to flight at a series of increasing speed waypoints until the structural instabilities are detected from the acquired flight data. Thus efficient and effective flutter prediction methods utilizing the test data are in demand to speed up the actual test without a loss of safety. Different approaches about flutter prediction are discussed later in Section 1.3.

## 1.2. Features of Mini-Launcher

A mini-launcher is a less than 100 kilograms rocket able to put small payload in Low Earth Orbit (LEO) like a Cubesat or a swarm of femto-satellites. By definition, this kind of devices are low cost and they are forced to use Micro-Electro-Mechanical Systems (MEMS).

A construction of a mini-launcher follows the *Space Payload Paradigm*[10] where the manufacturing cost of this mini-launcher is so low that it is feasible to build a launcher scaled to the payload if the payload controls the launcher. The interest in the current work is focused in the technology used for this kind of mini-launchers.

When flutter study is carrying out, there is a scale effect for this kind of design. This is because the size of MEMS are comparable to the size of the launcher. Typical sizes for MEMS are few millimeters while the size of the launcher is few centimeters. For our purpose, selection of adequate sensor distribution to measure the flutter is desired in order to not modify the real modes of final design. In this sense the only way to have the same result between the development phase and the real flight phase is to have always these sensors inside the structure as a part of the design. This is why a prediction using the data-based parameter-varying model is one of the most adequate in the design phase.

We have selected the ST Microsystem LIS331HH accelerometer. This is a $3x3\,mm$ in size that is comparable with the launcher size in about 5% which is $D145x55\,mm$. Main Control Unit (MCU) is adopted, which is an *Arduino Pro Mini* board, power supply of $5\,V$ at $16\,MHz$ of CPU clock which is the *Atmega168* with $32\,kb$ of memory. There was not feasible to store the information of each test so we decided to send in real time to the ground station. This technique will simplify the design. In one hand the mass of on-board sensors will be small and the other hand, in case we lose the launcher, we will not lose the data.

The sensor distribution designed in the begining was to put three accelerometers inside the ablative material, the cylinder layer between the inner cylinder that is the propellant

and the outer cylinder that is the structure. The wiring of the accelerometer[2] LIS331HH is displayed in figure 1.3. The use of a PCB board reduces the implementation time and improves the accuracy but opposite, it increases the size from $3\,mm$ to $6\,mm$ that represents 11% of the launcher size. Other good option is to use the Inertial Measurement Unit (IMU) from the femto-satellite. In chapter 4 we will discuss the experiment setup in detail and why we decided to use only the IMU instead of a net of sensors.

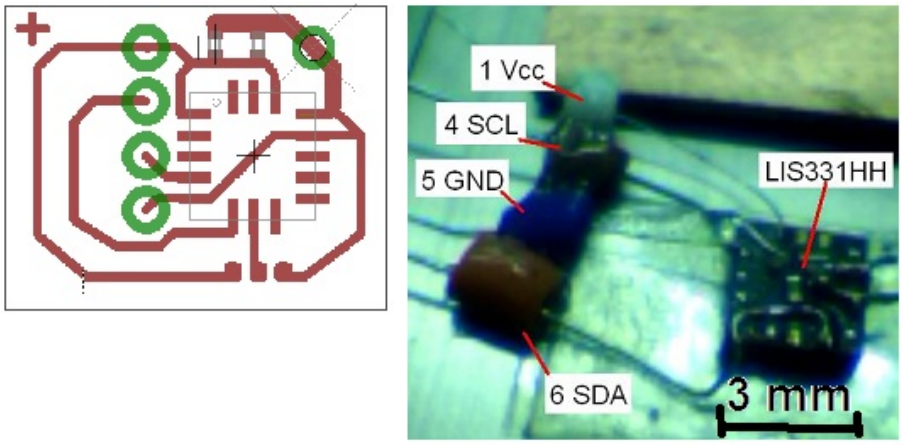


Figure 1.3: LIS331HH Accelerometer. Breadboard and wiring implementation

Other important effect that is different from common aircrafts is the absence of atmosphere. It does not mean that there is not an aerodynamic influence in the flutter, but these aerodynamic forces are not coming from the outside of the launcher but from the inside. Solid propellant combustion area generates an accelerating high pressure, high temperature flow towards the nozzle and vibration modes appears in the walls of the launcher.

### 1.2.1. Special features

This kind of mini-launcher are made by definition with low cost materials. For this reason the structure is made with domestic materials that were not originally designed for space applications but were validated for space later on. Most of these materials are: Aluminum sheets, Steel cans, Fiberglass, Epoxy, etc. In the flutter prediction, these huge range of Young Modulus (Elastic coefficient) is taken into account. Mini-launcher structures are based on a pressurized vessels. Any launcher stage is based on a can or a spray cylindrical container or something that can be reused. This kind of structures are mono-coke where inside there is a high pressure when it burns and no pressure the remaining time. This configuration makes the structure very strong against the thrust loads and torsion moments. The main difference respect to ordinary rockets is that many components are glued with epoxy instead to use any common joint like rivets, lock pins or bolts. The size of the smaller bolt available in the domestic market is to large for mini-launchers. Flutter phenomena can be very destructive for glued attachments.

[2] http://www.st.com/stonline/products/literature/ds/16366.pdf

### 1.2.2. Launch scenarios

The scenarios for mini-launchers are very often near-space, they have their lift-off from a balloon, also known as *Rockoon*, rather than being immediately lit while on the ground. Instead, they are carried into the upper atmosphere by a gas-filled balloon, then separated from the balloon and automatically ignited. The selected technique for the Wikisat group is based on a PVC tube connected to the balloon and it was designed by Lluis Bonet[11]. The pressure inside the balloon and the helium atmosphere is connected to the launching ramp where the launcher stays in armed mode. Near the burst moment, the launcher ignites and a fast shock wave is propagated towards the stressed balloon that provokes an imminent burst. Few milliseconds after, the launcher crosses through the weak helium atmosphere and starts the trajectory towards the space in high vacuum. In this kind of physical conditions, the mini-launcher structure should deal with shock waves which are high but having time to time short peaks of temperature, flames and fast changes in pressure and types of atmospheres. For the rest of the trajectory, the structure deals with high accelerations (In the range of hundreds of $g$) until the moment to jettison and second stage ignition.

### 1.2.3. Design Concept

In figure 1.4 there is an example of mini-launcher based on common and domestic containers. The left hand can is the fairing, the large can is the first stage and the right hand can is the second stage the one we want to study in deep. This is the so called *Wiki-Launcher* version $1$ that has two stages and femto-satellites are placed around the second stage. The first stage which is the lower one is to achieve an apogee of $250\,km$ and the second stage which is a coke can is to reach the required orbital speed of about $8\,km/s$ parallel to the ground.


Figure 1.4: a) WikiLauncher Boom View and b) WikiLauncher version 1

Based on Esteve Bardolet[12] calculations and using the same tool called *Moon2.0* simulator[3], the first stage burn-out is about $20\,s$ then 4 minutes later, the second stage burns for about $2\,s$. In terms of accelerations, the first stage acceleration peak is about $40\,g$ and the second stage acceleration peak is about $300\,g$ as shows the figure 1.5.

[3] http://code.google.com/p/moon-20/

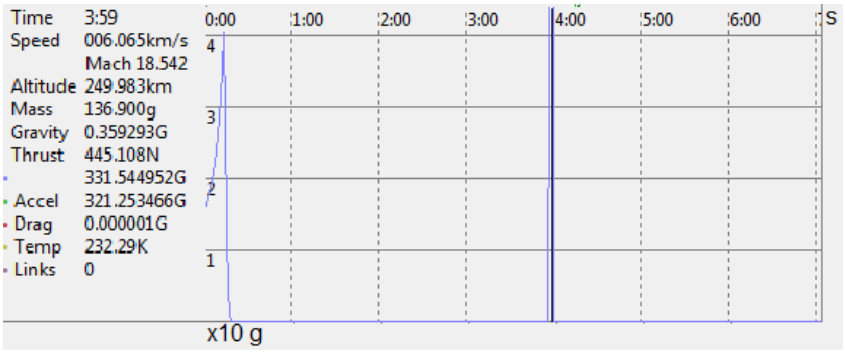


Figure 1.5: Thrust vs time graph for the Wiki-Launcher

In this thesis we are interested in the second stage because it is the most demanding situation that this kind of structures should resist. The size of the second stage is based on a $330\,ml$ steel commercial long coke that has about $400$ grams of solid propellant. The propellant used is Ammonium Perchlorate Composite Propellant (APCP) that is in the center of the container with a inner hole. This propellant burns from the inner diameter towards the outer diameter. Between the steel coke and the propellant there is a cylinder of epoxy that works as an ablative material in order to consume the heat during the burn, avoiding the melting point of the steel, keeping the best performances of this material while cool. The size as showed in figure 1.4 is about $120\,mm$ in length and $55\,mm$ in diameter.

Also we are very interested in the aerodynamic effects in the vacuum and how inner flow affects to the flutter. For this reason, firstly it is necessary to know well the behavior of the launcher without inner flow in order to see what is the source of vibrations and what are the modes. Later on, adding the inner flow, it is possible to study the flutter and its limits. Traditional wind tunnel studies are required for the launcher behavior, basic parameters like drag coefficient, lift coefficient and moment coefficient as a function of the angle of attack, the harmonics for each speed even in subsonic and supersonic speeds. The solid propellant has a changing geometry that generates a changing flow; the simulation and the study of this changing flow respect to the time is quite complicated. The prediction using the data-based parameter-varying model allow us to skip this hard study with few experiments.

## 1.3. Challenge for Flutter Prediction

### 1.3.1. Comparison of Flutter Prediction Methods

As shown in Section 1.1, flutter always raises new challenges to high-performance flight vehicles. It is essential to make sure the vehicles are flutter free. Thus plenty of flutter prediction methods are developed from theoretical analysis and engineering convention. Generally, flutter prediction methods can be classified into two major categories, model-based and data-based approaches. Model-based approaches usually requires to build the finite element model of the aeroelastic system; and then with some simplification hypothesis, theoretical or engineering calculation algorithms are used to obtain the critical flutter

condition. Data-based approaches means to rely on the test data to predict the flutter boundary.

There are many traditional data-based methods to predict the onset of flutter during flight testing[1], such as Modal Damping Extrapolation[2], Envelope Function and Flutter Margin (Zimmerman-Weissenburger method)[3], etc. The advantage of the data-based methods is that it requires little model information and is easy to handle, but the shortcomings are also obvious. Due to the rather noisy test data and various flutter mechanics, simply to extrapolate the indicating parameters extracted from test data for the critical flutter point may be biased. The left diagram in figure 1.6 illustrate the key problem of using the damping as an indicator of flutter, which is dependent on the types of flutter. The extrapolation may only work for mild flutter, and can hardly be used for explosive flutter. The right diagram in figure 1.6 shows a typical plot for Z-W Method, the selected stability parameters - flutter margin $FM$ fits well as a quadratic polynomial variation with the dynamic pressure $q^i$, that is

$$FM = f_{m2}(q^i)^2 + f_{m1}q^i + f_{m0} \tag{1.2}$$

where $f_{mi}$ are coefficients to be estimated from data taken from series of test waypoints. It is proved that the curve of $FM$ remain this tendency even for explosive flutter. Thus the prediction is to find the critical dynamic pressure when $FM = 0$. But the flutter margin $FM$ is derived based on a two-degree-of-freedom analysis, which means this Z-W method is mainly for a binary system, or 2-DOF flutter.

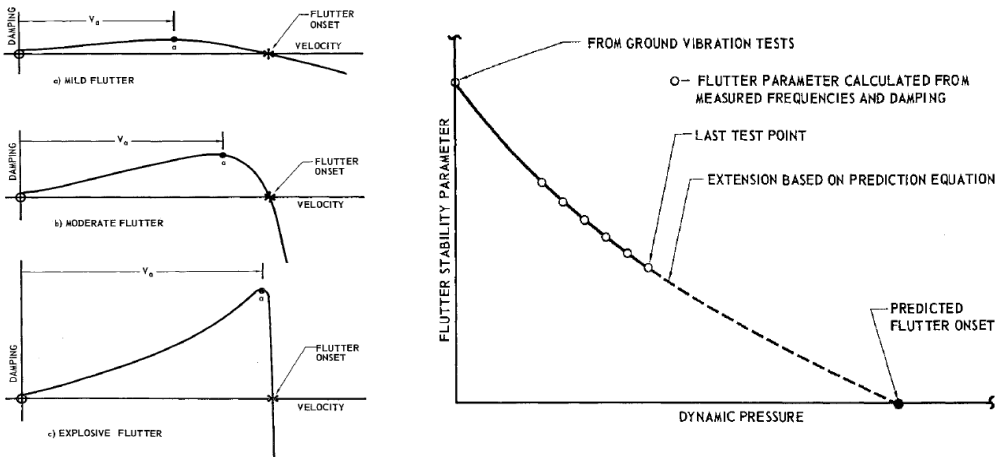


Figure 1.6: Typical Plots for Damping Extrapolation and Z-W Method Prediction [3]

Then a model-based $\mu$ method approach combining system model and flight data is proposed, the idea of robust flutter boundary prediction is shown by figure 1.7. One of the applications is on-line prediction tool-the flutterometer[4]. With the initial finite element and aerodynamics as the nominal model ($P$) unchanged, only the uncertainty operators ($\Delta$) of the robust aeroelastic model are updated using the test data. With both information, the Structured Sigular Value ($\mu$) is calculated as an indicator of the system stability. The flutter bounds depend heavily on the estimation and validation of the uncertainty. Match-point solutions are derived for robust flutter analysis[5].

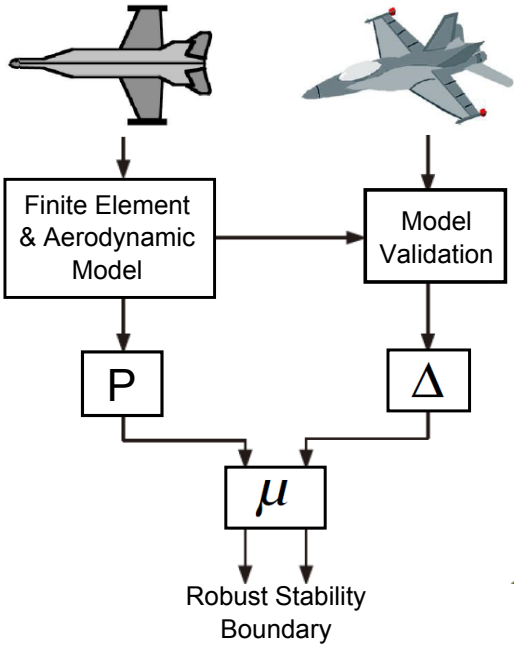


Figure 1.7: Idea of Robust Flutter Boundary Prediction

### 1.3.2. Discussion about Mini-Launcher Flutter

There remains plenty of blank about flutter of Mini-Launcher. Mini-Launcher itself is a relatively new area. Because of the unique mini design characteristics, different material and structure from ordinary launcher, the research about its flutter feature is rather attractive and challenging.

Nowadays, panel flutter is playing a more and more important role in the category of flutter since 1945. The outer surfaces of the vehicles are divided by internal structures into individual panels which may suffer from an unstable oscillation well-known as panel flutter.[17]

Usually as a consequence of supersonic flight, those outer surfaces of supersonic airplane or missiles which are not designed to hold primary structural loads, for instance fairings to control surfaces, are often too thin to sustain the loads and prone to fall into flutter, thus panel flutter criterion become the main consideration for such panels. Sometimes influence of the aerodynamic heating increase the possibility of panel that suffer from compressive loads to flutter, since large thermal stresses may arise.

The calculation of panel aerodynamics in high supersonic flight is adequate to use Piston Theory. But for aerodynamic analysis of cylindrical shells, the validity of Piston Theory is in doubt, where significant changes in aerodynamic pressure and phase have been reported.

The stability analysis for cylindrical and conical shells have to rely on lots of assumptions, like an infinitely long isotropic cylinder, inviscid flow, etc. Thus it seems the analysis is incapable of predicting accurately flutter observed from experiments. And as for the mini-launcher, the internal flow due to the burning of propellant, may causes a problem similar like panel flutter, which may be a concern for Wiki-Launcher.

## 1.4. Proposed Solutions

It is difficult to find out what kind of flutter or aeroelastic unstable may occur unless doing experiments. On the other hand, theoretical analysis for panel flutter has not been well-developed yet. Direct calculation is difficult. That's the reasons why to choose experiment methods and to apply a relatively new method, focusing on a data-based parameter-varying model, for flutter prediction. The flutter boundary of a mini-launcher may be predicted using a data-based airspeed-dependent parameter-varying model, with the well-developed linear fraction transform (LFT) and $\mu$-analysis as the core algorithms. Compared with the former model-based robust $\mu$ method incorporating test data into model, this approach requires less model information, besides it is usually more convenient to handle and takes less time and efforts without a loss of validity. More detail about the algorithms and implementation of data-based $\mu$ method are given in Chapter 2.

# CHAPTER 2. FLUTTER PREDICTION APPROACH

In this work, the data-based parameter varying estimation (PVE) flutter prediction approach is the proposed solutions for mini-launcher. With the well-developed linear fraction transform (LFT) and $\mu$-analysis as the core algorithms, it requires less model information but is considered to be very effective. In this Chapter, the whole procedure of the PVE approach and the related algorithms are explained in brief. At the end, as a summary, three stages for how to implement the approach are illustrated.

## 2.1. Informative Test Data Acquisition

As the first step of the test, the structure model is excited by internal excitation (on-board excitation equipment) or external excitation (atmospheric turbulence, for instance) and the vibration responses are recorded. Then the data will either send back to the ground station simultaneously or save in an on-board device. The common way for test data gathering is illustrated by figure 2.1.

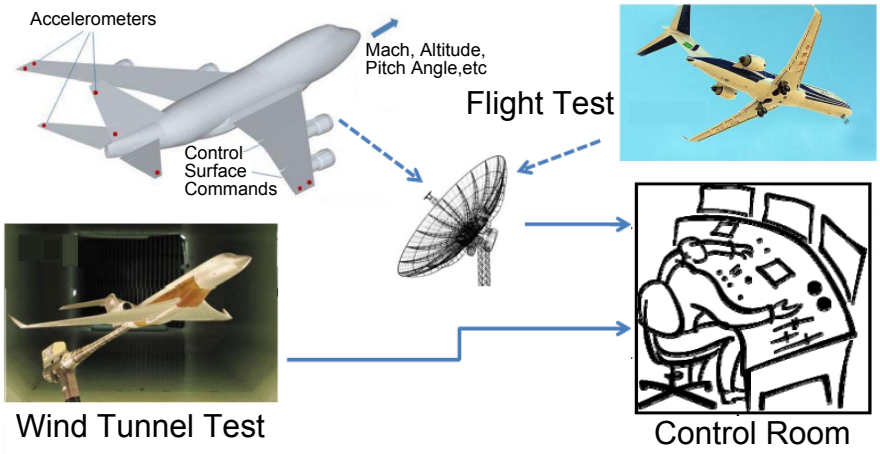


Figure 2.1: Test Data Gathering

The recorded test data is always corrupted with noise, and usually the Signal-to-Noise Ratio (SNR) is very low. Sometimes the test time is limited, thus only short-duration data is available, raising the difficulty of modal identification. Efforts are made to perform properly informative tests and improve the quality of the recorded data.

## 2.2. Modal Parameter Estimation

Modal parameter extraction is a foundational part of flutter prediction. It is made it in order to identify the modal frequencies and damping ratio of the critical aeroelastic modes. This step can be seen as one of the critical points as the final prediction results are very

sensitive to these identified modal parameters. According to whether the input signals are measurable or not, Model Parameter Estimation can be divided into Experimental Modal Analysis (EMA) and Operational Modal Analysis (OMA). With measured exciting signals and vibration response of the structures, EMA is used to study the characteristics of the structure model, usually based on the Frequency Response Function (FRF) data.

And OMA is a relatively new approach, which only measures vibration responses under operational circumstance, and the excitation sources, which may be the gust or turbulence, remain unknown. The advantage of OMA is that it adheres to the real operational conditions, which means a more realistic representation of the model.

Poly-reference Weighted Least Squares Complex Frequency-domain estimator (p-LSCF), one of the most popular and efficient identification methods, also known as *PolyMAX* method[18], is adopted here. The algorithms are based on the identification of right matrix fraction polynomial models:

$$H(\omega) = [B(\omega)][A(\omega)]^{-1} \tag{2.1}$$

The coefficients of the matrix polynomial are derived by minimizing the cost function and choosing proper parameter constraint. Then poles information or complex solutions can be induced from the denominator efficients. The secret of clear stabilization diagrams lies in the selection of parameter constraint[19]. From the stabilization diagrams, the physical mode information (modal frequency and damping ratio) is obtained.

## 2.3. Parameter-Varying Model Prediction

### 2.3.1. Block-Oriented Identification

Block-oriented nonlinear models consist of the interconnection of linear time invariant (LTI) systems and static (memoryless) nonlinearities. Hammerstein model and Wiener model are two types of the most frequently used block-oriented model. The Hammerstein model, consisting of the cascade connection of a static nonlinearity and a LTI system, shown as figure 2.2, can represent an actuator nonlinear effect, providing consistent estimates even with the colored output noise and less relying on the persistence of the input excitations[20]. The Wiener model, in which the order of the two components is reversed, is usually used for the sensor nonlinearity situation. In the following section, the Hammerstein model is considered, and non-iterative identification algorithms[21] are adopted, based on least square estimation and singular value decomposition.

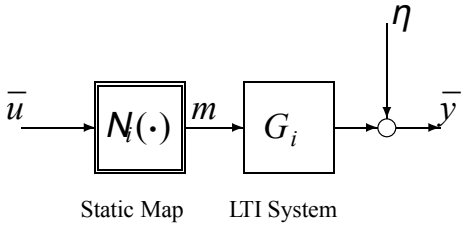


Figure 2.2: Hammerstein Model (Actuator Nonlinearity)

The nonlinear static operator $N(\cdot)$ can be parameterized by polynomial or cubic spline function[22]. The LTI system is described by its transfer function,

$$G(q) = \sum_{l=0}^{p-1} b_l B_l(q) \tag{2.2}$$

$q$ is the forward shift operator, $b_l$ are the matrix parameters to be estimated, and $B_l(q)_{l=0}^{p-1}$ is the set of orthonormal bases, tuned with the modal parameters information identified from the test data. Based on balanced realizations of all-pass functions, a unifying construction of orthonormal bases[23] is used to incorporate the chosen poles at $\{\xi_0, \xi_1, \cdots, \xi_{p-1}\}$.

$$B_n(q) = \left( \frac{\sqrt{1-|\xi_n|^2}}{q-\xi_n} \right) \sum_{k=0}^{n-1} \left( \frac{1-\bar{\xi_k} q}{q-\xi_k} \right) \tag{2.3}$$

Complex modes should be included in conjugate pairs. Then the input-output relationship is given by

$$\bar{y}_k = G(q)N(\bar{u}_k) + \eta_k \tag{2.4}$$

Now, with the measured data set $\{\bar{u}_k, \bar{y}_k\}_{k=1}^N$, an estimate of parameters can be computed by least-squares criterion and singular value decomposition.

### 2.3.2. Parameter-Varying Estimation Model

At each waypoint $i = V_0 \in [V_{lower}, \cdots, V_{upper}]$, a LTI system is estimated as above, then transformed to its state-space minimal realization. The velocity dependency is included by fitting the identified system to a quadratic or cubic matrix polynomial function of the velocity $(j = 2 \; or \; 3)$:

$$\bar{P}_i = \begin{bmatrix} A^i & B^i \\ C^i & D^i \end{bmatrix} \simeq \begin{bmatrix} \hat{A}(V^i) & \hat{B}(V^i) \\ \hat{C}(V^i) & \hat{D}(V^i) \end{bmatrix} = \begin{bmatrix} A_0 + A_1 V^i + A_2 (V^i)^2 & B_0 + B_1 V^i + B_2 (V^i)^2 \\ C_0 + C_1 V^i + C_2 (V^i)^2 & D_0 + D_1 V^i + D_2 (V^i)^2 \end{bmatrix} \tag{2.5}$$

The parameter-varying estimation model[6] is thus constructed by including a velocity perturbation $\delta_V^i$

$$V^i = V_0 + \delta_V^i \tag{2.6}$$

where $V_0$ is the $i$-th waypoint's velocity. Thus the interconnection between nominal model $\bar{P}^(2)(V_0)$ and a new set of feedback signals $z_j, \omega_j$ is shown in figure 2.3 .

Making use of the linear fraction transform[7], the former state-space expression $\bar{P}_i$ is equally parameterized to be a velocity dependent model:

$$\bar{P}_i = F_l[\bar{P}^{(j)}(V_0), \delta_V^i] \tag{2.7}$$

Then flutter prediction will just focus on searching for the lowest velocity perturbation leading to the critical flutter point.

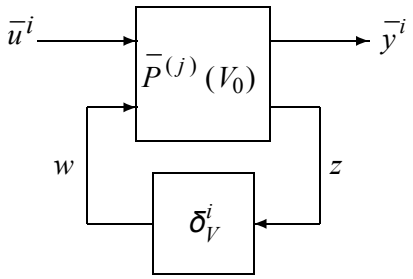


Figure 2.3: $\mu$ Analysis Model (Velocity-dependent)

### 2.3.3. $\mu$ Analysis Prediction

According to perturbation theory[7], the critical perturbation to velocity lemma states that:

$$\delta = min\{\delta_q^i > 0 : F_l[\bar{P}^{(j)}(V_0), \delta_V^i] \ is \ \ unstable\}, \ \ (j = 2 \ or \ 3) \tag{2.8}$$

The structured singular value:

$$\mu(\bar{P}^j) = \frac{1}{\delta}$$

The nominal flutter speed:

$$V_f = V_0 + \delta$$

So by iterating over the velocity, a critical value of $\delta_V^i$ may be found when one of the eigenvalue of the state matrix of $F_l[\bar{P}^{(j)}, \delta_V^i]$ has a positive real part, and the system becomes unstable.

## 2.4. Implementation Procedure

As a summary of the flutter prediction approach and algorithms discussed above, the implementation procedure is divided into three stages, as shown by figure 2.4.

**1. Test Data Acquisition**

The preparation for a flutter test includes the configuration of excitation and sensors, the parameters of sensors, test environment and so on. The length of the recorded data should be long enough for further process, and disturbing noise incorporated in the recorded data should be as little as possible.

**2. Modal Identification**

To improve the accuracy of modal parameter extraction, some pre-processes may be used to help raising the SNR of test data. Modules from the commercial software-LMS Test.Lab, produced by a successful leading company in modal tests named LMS [1], is applied here. The inputs to these PolyMAX modules can either be time domain data or frequency domain (FRFs) data. For time domain response inputs, OMA method is adopted, corresponding

[1] http://www.lmsintl.com/

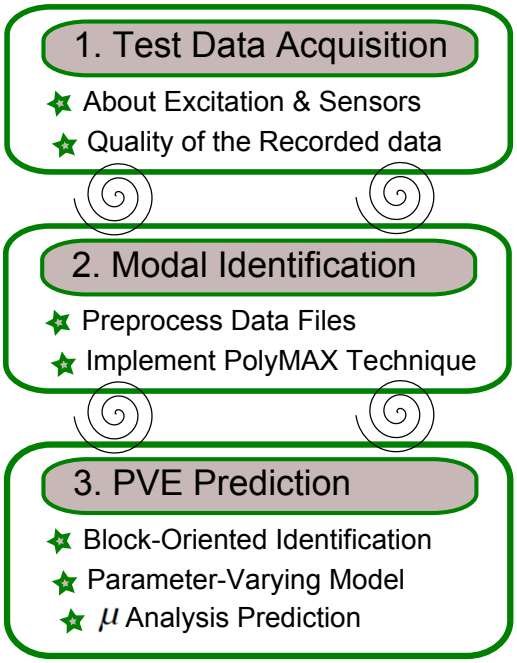


Figure 2.4: Implementation Procedure of Parameter-Varying Prediction

to Op.PolyMAX Module from LMS Test.Lab. And for FRF inputs, EMA method is eligible, which is relative to PolyMAX Module from LMS Test.Lab. A Data Format Convert interface is designed using MATLAB GUI program. Thus it can convert the time or frequency domain data files into compatible formats (Universal File Format, UFF58) for PolyMAX Identification in batch processing, with the convert interface showed in figure 2.5. Then a glimpse of the PolyMAX Module is given by figure 2.6. The use of Automatic Selection to select stable poles leads to a rapid selection and repeatable identified results.

**3. Parameter-Varying Prediction**

Referring to the algorithms in Section 2.3, 2.3.3, and using MATLAB M-File as the program language, the prediction approach is implemented to estimate flutter boundary. And two typical application cases used for verification are given in the following Chapter.

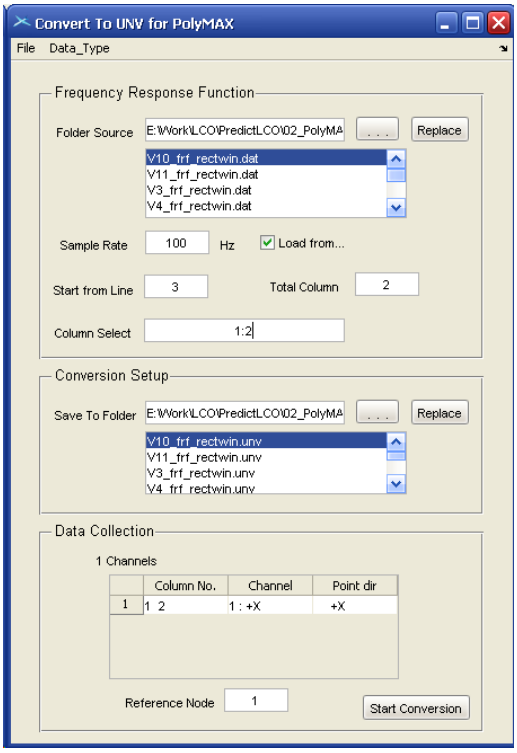


Figure 2.5: Interface of the Format Convert Program

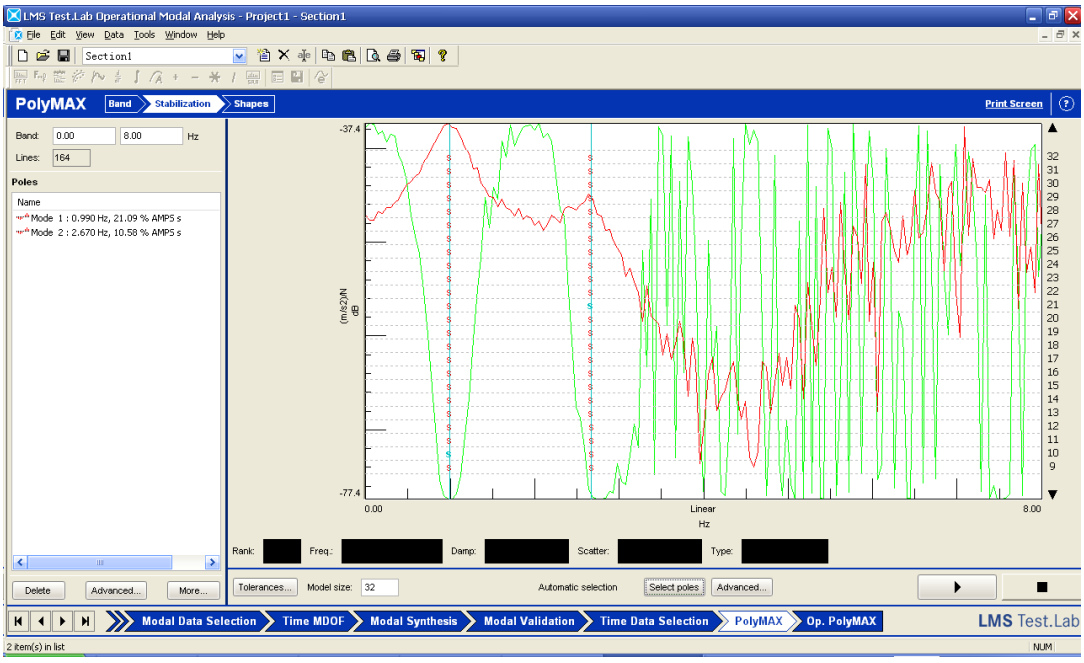


Figure 2.6: Stabilization Diagrams from PolyMAX Module

# CHAPTER 3. APPLICATION CASES

Before to use the aforementioned method in mini-launchers, two typical flutter prediction scenarios are illustrated in this chapter in order to validate the method. One is a prototypical plunge-pitch Aeroelastic system with simulated data, and the other one is a scaled aircraft half-model for dynamic aeroelastic study, providing a great amount of real wind tunnel test data ready for the study of flutter prediction. Thus it is focused on demonstrating the validation of PVE data-based flutter approach using these application scenarios, which would be a good foundation for the implementation of mini-launcher.

## 3.1. Prototypical 2-Dimensional Aeroelastic System

### 3.1.1. Model configuration

A prototype aeroelastic model is presented in figure 3.1

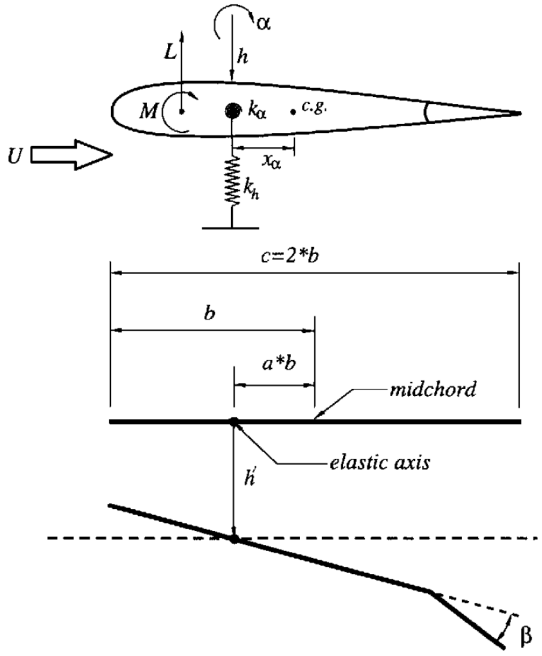


Figure 3.1: A Prototypical Aeroelastic Model [24]

The system parameters are listed in table 3.1

### 3.1.2. Direct Simulation

As a prototypical aeroelastic system, the DOFs is simplified to be pitch and plunge, represented by pitch angle $\alpha$ and plunge parameter $h$. Thus the system equation of motion is

Table 3.1: Prototypical System Parameters

| **Geometric Parameters** | | **Inertial Parameters** | |
|---|---|---|---|
| Semichord $b$ | 0.135 $m$ | Mass $m$ | 12.387 $kg$ |
| Elastic axis $e$ | -0.6 | $x_\alpha$ | 0.2466 |
| **Damping Parameters** | | $I_\alpha$ | 0.065 $kg \cdot m^2$ |
| $c_h$ | 27.43 $kg/s$ | **Aerodynamic Parameters** | |
| $c_\alpha$ | 0.180 $kg \cdot m^2/s$ | $c_{l_\alpha}$ | $2\pi$ |
| **Stiffness Parameters** | | $c_{m_\alpha}$ | -0.628 |
| $k_h$ | 2844.2 $N/m$ | $c_{l_\beta}$ | 3.358 |
| $k_\alpha$ | 2.82 $N \cdot m/rad$ | $c_{m_\beta}$ | -0.635 |

described by

$$\begin{bmatrix} m & mx_\alpha b \\ mx_\alpha b & I_\alpha \end{bmatrix} \begin{pmatrix} \ddot{h} \\ \ddot{\alpha} \end{pmatrix} + \begin{bmatrix} c_h & 0 \\ 0 & c_\alpha \end{bmatrix} \begin{pmatrix} \dot{h} \\ \dot{\alpha} \end{pmatrix} + \begin{bmatrix} k_h & 0 \\ 0 & k_\alpha \end{bmatrix} \begin{pmatrix} h \\ \alpha \end{pmatrix} = \begin{pmatrix} -L \\ M \end{pmatrix} \quad (3.1)$$

Where $c_\alpha$ and $c_h$ are the structural damping coefficients for pitch and plunge, $k_\alpha$ and $k_h$ are the corresponding stiffness parameters. The values of the system parameters are given in Table 3.1. The quasi-steady expressions for aerodynamic force $L$ and force moment $M$ are

$$L = \rho V^2 b c_{l_\alpha} \left[ \alpha + \frac{\dot{h}}{V} + (\frac{1}{2} - e) b \frac{\dot{\alpha}}{V} \right] + \rho V^2 b c_{l_\beta} \beta \quad (3.2)$$

$$M = \rho V^2 b^2 c_{m_\alpha} \left[ \alpha + \frac{\dot{h}}{V} + (\frac{1}{2} - e) b \frac{\dot{\alpha}}{V} \right] + \rho V^2 b^2 c_{m_\beta} \beta \quad (3.3)$$

where $c_{l_\alpha}$ and $c_{m_\alpha}$ are the lifting and lifting-force moment coefficients to attack angle $\alpha$, and $c_{l_\beta}$, $c_{m_\beta}$ are the lifting and lifting-force moment coefficients to flap rotation $\beta$.

Derived from these equations, the simulation for the system responses is set up as figure 3.2, using Matlab Simulink module.

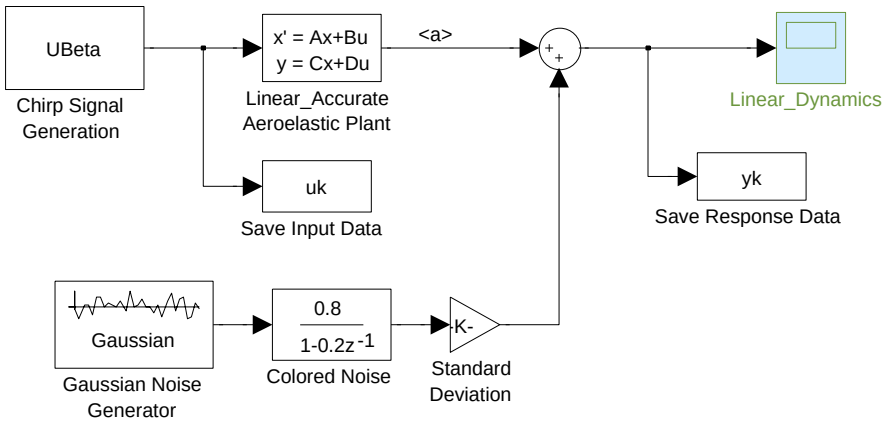


Figure 3.2: Simulink Diagram for Aeroelastic System Simulation

The system output is the pitch angle $\alpha$, corrupted with 0-averaged Gaussian distribution white noise. The input is the flap rotation $\beta$, which has been the linear swept signal from $0.0Hz$ to $5.0Hz$ within 32 seconds at an amplitude of 10 degrees. The sample rate for data

acquisition is $100\,Hz$. The direct simulation results for flutter is $12.11\,m/s$ at a frequency of $2.11\,Hz$. The response of pitch angle at several speed points are shown on figure 3.3.

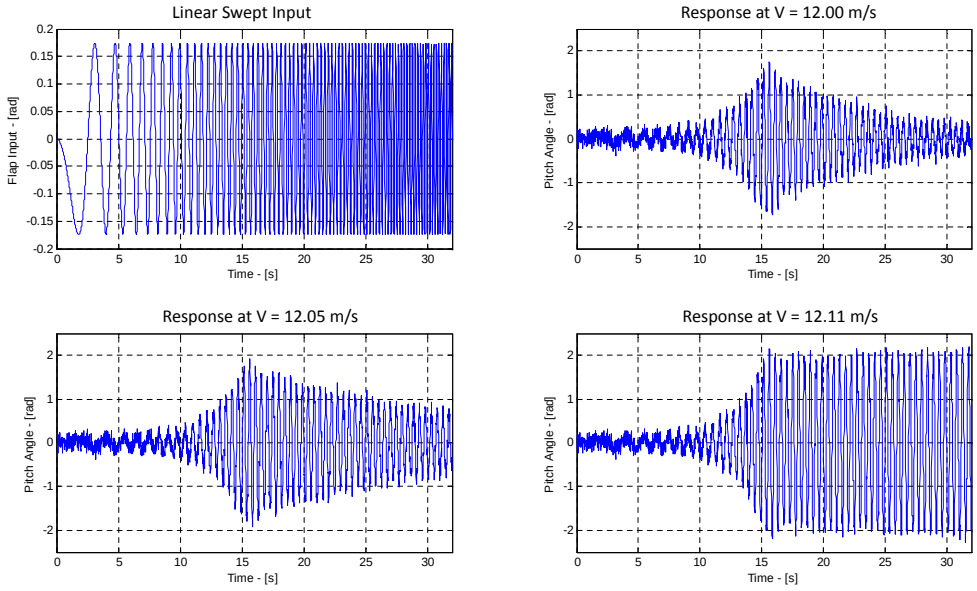


Figure 3.3: Linear Dynamic Responses to Swept Sine Input

### 3.1.3. Flutter Prediction

#### 1. Simulated Response Data

In order to validate the parameter-varying flutter prediction approach, responses at several waypoints are simulated by Simulink, ranging from $V = 3.0\,m/s$ to $11.0\,m/s$, nine velocities in total, with an artificial noise level around SNR 8.9, which means a severe noise. All the input and output time-domain data are saved for PolyMAX Modal Identification. The poles information from direct simulation is also stored for further comparison.

#### 2. PolyMAX Modal Identification

Firstly from the input and output time-domain data, FRFs are calculated for PolyMAX identification, with a frequency resolution of $0.0488\,Hz$ and rectangle window added.

Then data format convert program is used to obtain the .UNV files that will be imported to PolyMAX Module to extract the poles parameters (modal frequency and damping ratio). The identified poles results are displayed in table 3.2.

#### 3. Flutter Prediction

From the identified poles information, the tendency of frequency and damping ratio respect to airspeed is plotted on figure 3.4, indicating a classical 2-dimensional coupling flutter.

figure 3.4 indicates a kind of 2-DOF (pitch and plunge) classical flutter, which may be suitable for some traditional flutter prediction methods. In this scenario, two kinds of other

Table 3.2: Comparison between real Poles and Estimated Poles Parameters

| Airspeed | **Theoretical real poles** | | | | **Identified poles from PolyMAX** | | | |
|---|---|---|---|---|---|---|---|---|
| $V^i$ | Mode No.1 | | Mode No.2 | | Mode No.1 | | Mode No.2 | |
| $m/s$ | $f, Hz$ | $\delta$, % | $f, Hz$ | $\delta$, % | $f, Hz$ | $\delta$, % | $f, Hz$ | $\delta$, % |
| 3 | 1.04 | 20.48 | 2.73 | 10.74 | 1.04 | 20.10 | 2.72 | 9.70 |
| 4 | 1.06 | 20.62 | 2.70 | 10.68 | 1.06 | 20.09 | 2.69 | 9.70 |
| 5 | 1.10 | 20.72 | 2.67 | 10.60 | 1.10 | 20.12 | 2.66 | 9.70 |
| 6 | 1.14 | 20.81 | 2.64 | 10.49 | 1.14 | 20.18 | 2.63 | 9.64 |
| 7 | 1.19 | 20.91 | 2.59 | 10.33 | 1.19 | 20.23 | 2.58 | 9.54 |
| 8 | 1.26 | 21.07 | 2.53 | 10.07 | 1.26 | 20.39 | 2.52 | 9.27 |
| 9 | 1.34 | 21.39 | 2.46 | 9.62 | 1.34 | 20.66 | 2.45 | 8.83 |
| 10 | 1.43 | 22.11 | 2.36 | 8.77 | 1.45 | 20.64 | 2.36 | 7.93 |
| 11 | 1.56 | 24.02 | 2.24 | 6.69 | 1.59 | 20.49 | 2.24 | 5.98 |

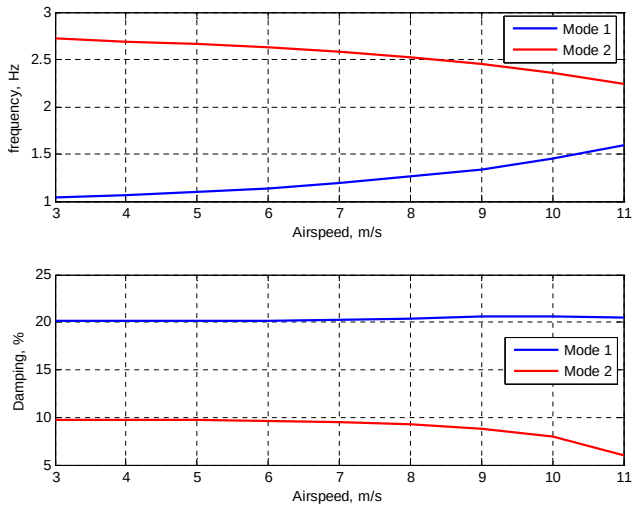


Figure 3.4: Trends of Frequency and Damping versus Airspeed

approaches, modal damping extrapolation and flutter margin (Z-W method) are also applied to compare with the parameter-varying estimation.

As traditional data-based methods, both the modal damping extrapolation and Z-W method simply rely on the identified poles parameters. The tendency of respective flutter indicators with airspeed or dynamic pressure is depicted in figure 3.5

The proposed parameter-varying estimation (PVE) approach is then applied to tune the poles information into prediction model. The flutter boundary is acquired from the stability analysis of identified model. Here quadratic and cubic function of dynamic pressure and airspeed are adopted separately, and also average results are calculated. The figure 3.6 shows the flutter speed and frequency results obtained utilizing the PVE model derived from function of quadratic and cubic dynamic pressure. A summary of the flutter prediction results are given in table 3.3 and 3.4.

From table 3.3, the disadvantage of damping extrapolation is obvious. The closer the waypoint goes to the critical point, the more accurate the prediction results will be. But it

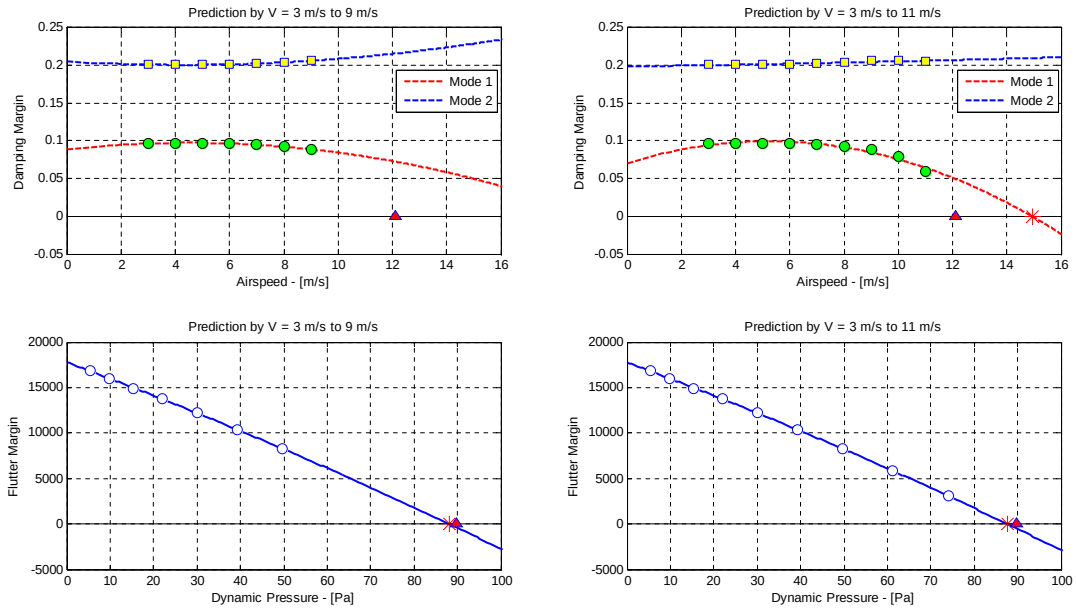


Figure 3.5: Damping Extrapolation and Flutter Margin Prediction

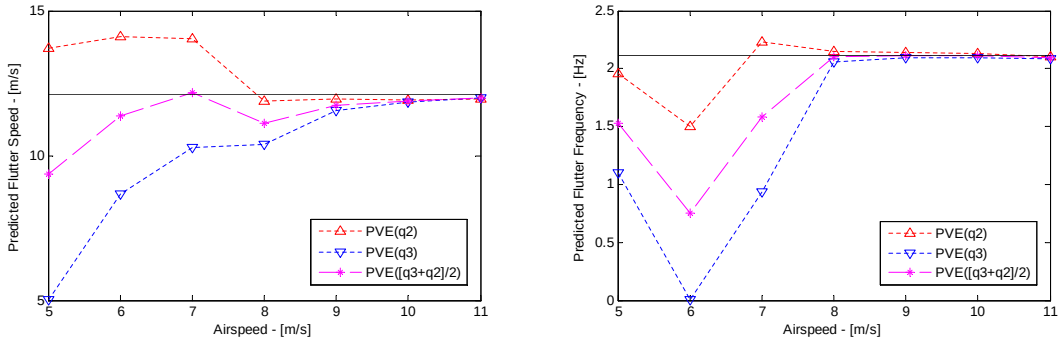


Figure 3.6: a) Predicted flutter boundary; b)Predicted flutter frequency

is dangerous to be too close to the flutter speed. And the extrapolation only use modal damping as an indicator, thus relies a lot on the identified poles and selected waypoints, and sometimes the waypoints far from the critical point may be misleading. On the other hand, Z-W method proved to be an effective method to have a consistent estimation even far from the flutter point. But it can only used in the scenario that happens to be 2-DOF coupling flutter. As an traditional engineering method since 1964, it can be used to compare with PVE prediction results.

The predicted results by PVE seems rather fit with the real results, even under a severe noise of SNR $8.9dB$. The PVE is capable of giving flutter boundary since low speed waypoints far from the critical points. With different variables, such as $(q^2)$, $(q^3)$, $(V^2)$, $(V^3)$, the results may be a little bit different, thus the average technique is adopted, which turns out to give a better predicted boundary.

Table 3.3: Flutter speed prediction - 2-DOF aeroelastic system with linear sweep sine excitation ($SNR \approx 8.9\,dB$)

| True flutter speed from direct simulation: $12.11\,m/s$ | | | | | | | | |
|---|---|---|---|---|---|---|---|---|
| Approach Waypoint | Damping extrapolate | Z-W method | PVE $(q^2)$ | PVE $(q^3)$ | PVE $\frac{q^2+q^3}{2}$ | PVE $(V^2)$ | PVE $(V^3)$ | PVE $\frac{V^2+V^3}{2}$ |
| $V = 3 \sim 5$ | N/A | N/A | 13.72 | N/A | N/A | N/A | N/A | N/A |
| $V = 3 \sim 6$ | 29.34 | N/A | 14.12 | 8.65 | 11.38 | N/A | 11.09 | N/A |
| $V = 3 \sim 7$ | 26.85 | 14.08 | 14.05 | 10.27 | 12.16 | 12.67 | 11.44 | 12.06 |
| $V = 3 \sim 8$ | 21.92 | 11.98 | 11.88 | 10.38 | 11.13 | 12.08 | 11.09 | 11.59 |
| $V = 3 \sim 9$ | 19.52 | 11.99 | 11.94 | 11.55 | 11.74 | 12.04 | 11.69 | 11.86 |
| $V = 3 \sim 10$ | 17.14 | 11.94 | 11.93 | 11.85 | 11.89 | 12.00 | 11.86 | 11.93 |
| $V = 3 \sim 11$ | 14.93 | 11.96 | 11.96 | 11.98 | 11.97 | 11.99 | 11.95 | 11.97 |

Table 3.4: Flutter frequency prediction - 2-DOF aeroelastic system with linear sweep sine excitation ($SNR \approx 8.9\,dB$)

| True flutter frequency from direct simulation: $2.11\,m/s$ | | | | | | |
|---|---|---|---|---|---|---|
| Approach Waypoint | PVE $(q^2)$ | PVE $(q^3)$ | PVE $[q^2+q^3]/2$ | PVE $(V^2)$ | PVE $(V^3)$ | PVE $[V^2+V^3]/2$ |
| $V = 3 \sim 5$ | 1.96 | 1.10 | 1.53 | N/A | 1.12 | N/A |
| $V = 3 \sim 6$ | 1.50 | N/A | 0.75 | 2.64 | N/A | 1.33 |
| $V = 3 \sim 7$ | 2.23 | 0.93 | 1.58 | 2.14 | 1.70 | 1.92 |
| $V = 3 \sim 8$ | 2.15 | 2.06 | 2.10 | 2.13 | 2.07 | 2.10 |
| $V = 3 \sim 9$ | 2.14 | 2.09 | 2.12 | 2.13 | 2.11 | 2.12 |
| $V = 3 \sim 10$ | 2.13 | 2.10 | 2.11 | 2.12 | 2.11 | 2.12 |
| $V = 3 \sim 11$ | 2.11 | 2.08 | 2.09 | 2.11 | 2.10 | 2.10 |

## 3.2. Scaled Aircraft Wind Tunnel Model

### 3.2.1. Model setup

A scaled half-model aircraft, as shown on figure 3.7, is designed by Aeroelasticity Group of Beihang University to study the aerodynamic instability phenomenon and to evaluate the control law for Gust Load Alleviation, as well as the flutter prediction approach. A series of relative wind tunnel tests were conducted in February, 2011. The real model in the wind tunnel is shown as figure 3.8.

The Finite Element Method (FEM), illustrated by figure 3.9 is applied during the design and modification of the aircraft model. The main modal is picked out as Table 3.5

The calculation through FEM also indicates which modal has taken part into the coupling for flutter. That is first and second order of wing's bending, first order of fuselage's bending and first order of wing's torsion modal when the engine isn't attached. While with the influence of engine, the flutter point changes a little, with the join of bending and torsion mode of engine.

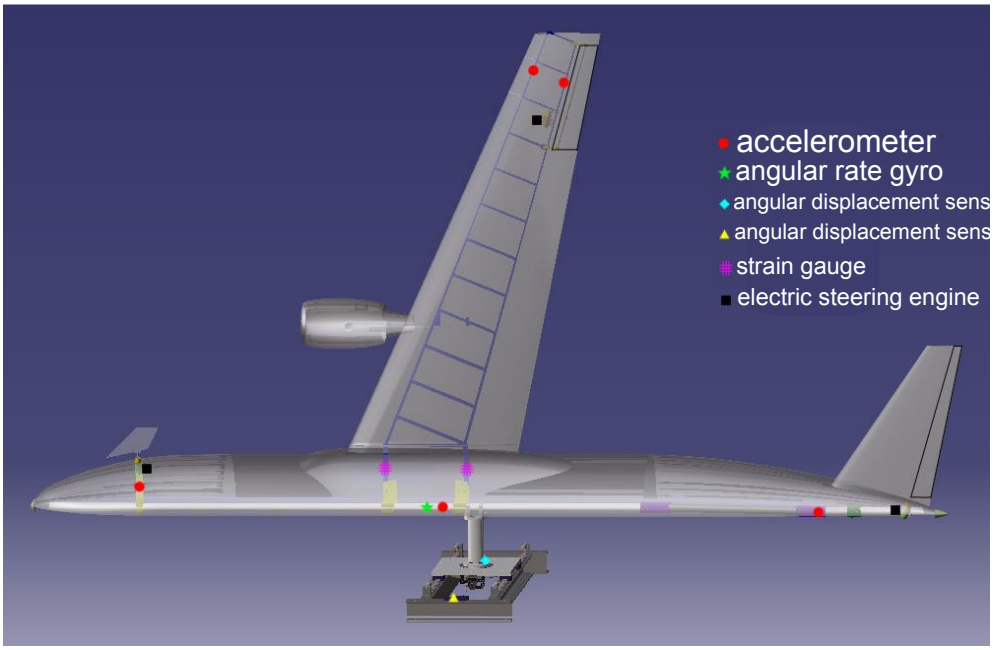


Figure 3.7: A scaled full-aircraft half model designed for aeroelasticity study

Table 3.5: Several major modes of the aircraft with or without engine

| **Aircraf model without engine** | Frequency, Hz | **Aircraf model with engine attached** | Frequency, Hz |
|---|---|---|---|
| 1st Bending of Wing | 1.72 | 1st Bending of Wing | 1.72 |
| 1st Bending of Fuselage | 5.33 | 1st Bending of Fuselage | 5.32 |
| 2nd Bending of Wing | 7.65 | 2nd Bending of Wing | 7.65 |
| 1st Bending of Stabilizer | 12.6 | 1st Bending of Stabilizer | 12.67 |
| 1st Torsion of Wing | 16.0 | 1st Torsion of Wing | 18.89 |
| | | pitch of engine | 11.38 |
| | | yawing of engine | 17.5 |
| FEM Calculation Result, flutter speed is $33.7 m/s$, at $7.1 Hz$. | | FEM Calculation Result, flutter speed is $31.5 m/s$, at $6.4 Hz$. | |

### 3.2.2. Tests for Flutter Prediction

From the FEM calculation results as Table 3.5, it is induced that the main modals of the aircraft are below $20 Hz$, thus the sample rate for DAQ is chosen to be $200 Hz$. And the step sin excitation is adopted fo have a more accurate information about FRF. Aileron, stabilizer and canard step sin excitation is implemented respectively, and all the important responses acquired by various sensors showed in figure 3.7 including the excitation data are acquired and saved to data files. The test scenarios related with flutter prediction consist of sweep sin start from $0.6 Hz$ to $7 Hz$, with a interval of $0.2 Hz$, and the test waypoints cover from $16 m/s$ to $29 m/s$ with sweep sin excitation, and later without excitation from $30 m/s$ to $33 m/s$ until the flutter critical point become so close. The results from wind tunnel test show a good corresponding to the FEM calculation. For the test with engine attached, it is similar, due to more modals coupling, the flutter speed is a bit lower, which is around $31 m/s$.

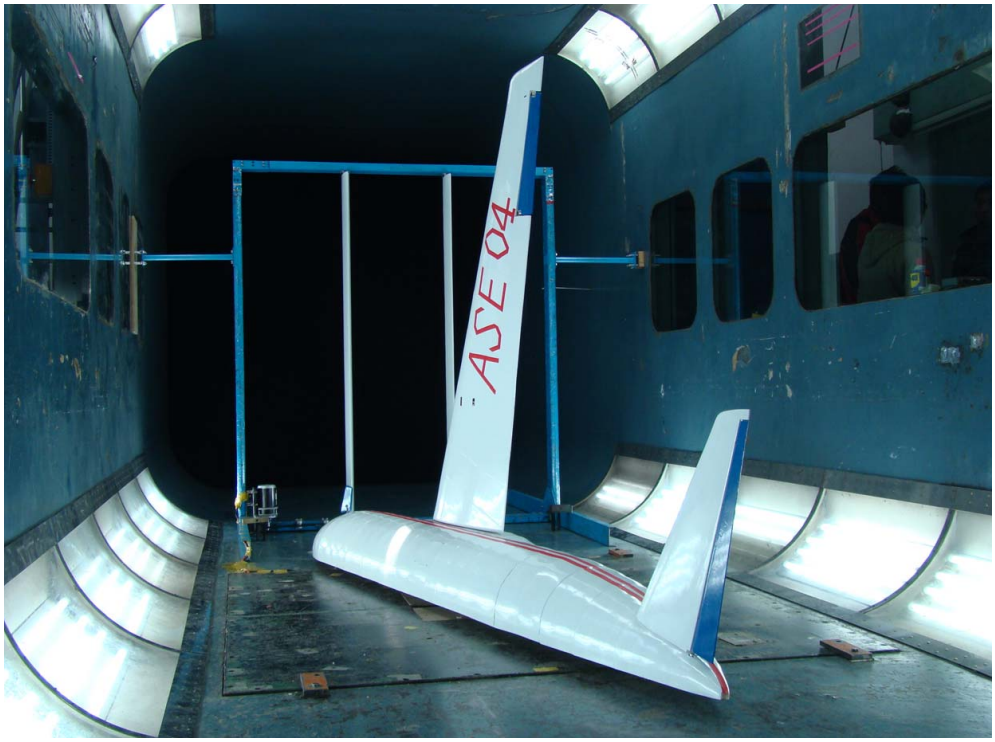


Figure 3.8: aircraft model called ASE04 under wind tunnel test

This aircraft model and wind tunnel test could be a rather good platform for the verification of prediction approach. Since it is almost like a real airplane, with more modals coupling, and the wind tunnel test data is always with much noise, somehow raised some difficulty for the the analysis and implementation of the PVE framework. But the main idea is clear, remaining only some small problems before we get the final prediction results. Now a brief summary of how the PVE data-based methods will be implemented to this aircraft model.

As there are always 10 channels of signals recorded at the time, such as the acceleration of fuselage at the center of gravity, at the nose, or at the wingtip. But it is always obvious that the response at the wingtip is much more informative that maybe served as the main output signal for further analysis. At $V = 22 m/s$, with an aileron step sine excitation, the response of wingtip is showed in figure 3.10. Since it is a step sine that lasts 4 seconds and rests $1$ second for each frequency. A data process method respect to step sine excited scenario maybe adopted to obtain a more accurate and rapid FRFs results. Then by fitting curves of FRFs with a discrete time transfer function, the poles of the critical modals are available, thus it goes to the similar procedure as Section 3.1.3. But as a real test model, many unexpected situation is possible, which requires a flexible adjustment.

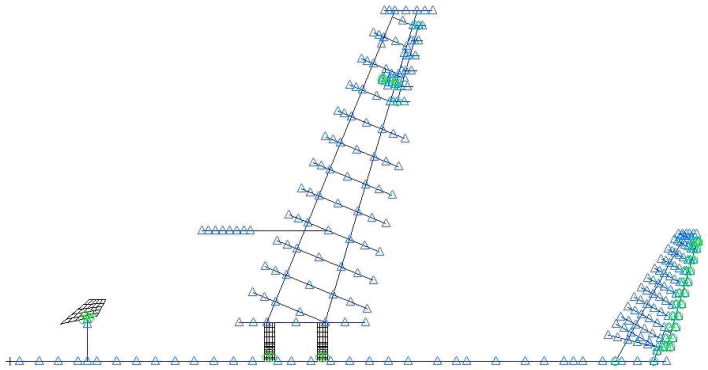

Figure 3.9: An aircraft model called ASE04 under wind tunnel test

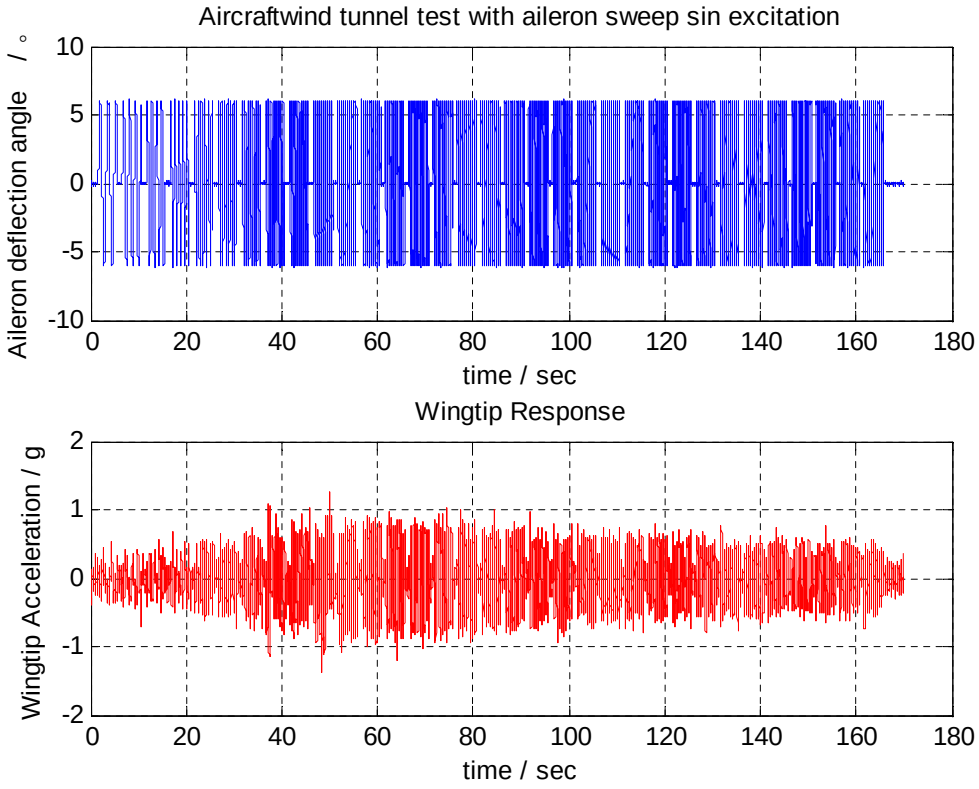


Figure 3.10: Aircraft wind tunnel test with aileron sweep sine excitation

# CHAPTER 4. WIND TUNNEL TEST

To study the flutter of a mini-launcher, subsonic or supersonic wind tunnel and launch tests are considered to acquire adequate informative test data. But one thing is clear that a scaled model for a mini-launcher may be too small to make. That why only the real size one is used. And also the sensors used inside of the launcher to measure the vibration should not influence the performance of the launcher. Luckily, as for the femto-satellite and the mini-launcher, an Inertial Measurement Unit (IMU) is always required for vector control of the launcher and satellite attitude determination. This means that we are not interfering in the launcher construction during flutter study. A sensor network is intended to be mounted inside the ablative material in the other part inside the structure but due to lack of time it was not realized. Then proper IMU was adopted to install inside the femto-satellite. In addition, real-time communication is connected between satellite and the ground station. Thus the telemetry may be used for flutter prediction. In this chapter, it includes four test items: wind tunnel speed calibration; aerodynamic parameters like Lift, Drag and Pitch moment as a function of the Angel of Attack (AoA) for a given wind speed; vibrations with varied angle of attack and airspeed; and finally responses with sweep sine excitation.

## 4.1. Preparation For the Test

For the basic aerodynamic test, two main tools are used, the wind tunnel and sensors. The wind tunnel allows us to change the flight conditions: the desired wind speed or the AoA. The sensors, mainly accelerometers will give us the responses in terms of vibration amplitude for a given direction. We can extend this study to the rotation which is another interesting vibration mode. It is obvious that the mini-launcher has a radial symmetric shape and the accelerometer has three axis, and when the AoA is changed, two of these axis are interchangeable. Vibrations in flight direction are not considered. These vibrations will be induced by the combustion flow during the burn but in our wind tunnel test only aerodynamics due to the wind is studied. Finally, there is one axis that does not change with the AoA and this is the axis selected for final process, otherwise the data should be rotated to the wind tunnel reference system. This simplified method is almost valid as the oscillation modes in any radial direction will be similar. The mini-launcher does not have asymmetric distribution masses because it consists of only cylindrical structures. One example of this is combustion section. The structure is a steel cylinder. The ablative material is a cylinder and inside of it there is the propellant that is also a cylinder. In the inner part is the combustion chamber that is still a cylinder. Any vibration mode should be similar in any radial direction. On the right of figure 4.1 shows the experiment setup in the wind tunnel and the axes orientation in which shows that the Z axis accelerometer will be the best to study the vibrations. Inside the Stage 2 of the Wiki-launcher there is a femto-satellite that has the sensors. This is the so-called Advanced Wireless Inertial Platform (AWIP) that it is used as a femto-satellite development kit[13]. The final WikiSat femto-satellite has a High Gain Antenna (HGA) but the rest is the same. For this test we are using the same source code as Victor Kracvhenko used.

Inside the AWIP the *ST Microsystems* LIS331HH 3 axis accelerometer is utilized. This is

a $3x3\,mm$ in size that is comparable with the size of mini-launcher which is $55\,mm$ in 5%. The femto-satellite development kit has a Main Control Unit (MCU) that is an *Arduino* like board. Power supply is $5\,V$ at $16\,MHz$ of clock frequency with an *Atmega168* as the CPU. The wiring of the accelerometer[1] LIS331HH is displayed in figure 4.1 at the left hand side. Additionally we use a *InvenSense* ITG-3200 3 axis gyro[2] with temperature sensor and a *freescale* MPL115A2 barometer[3] sensor.

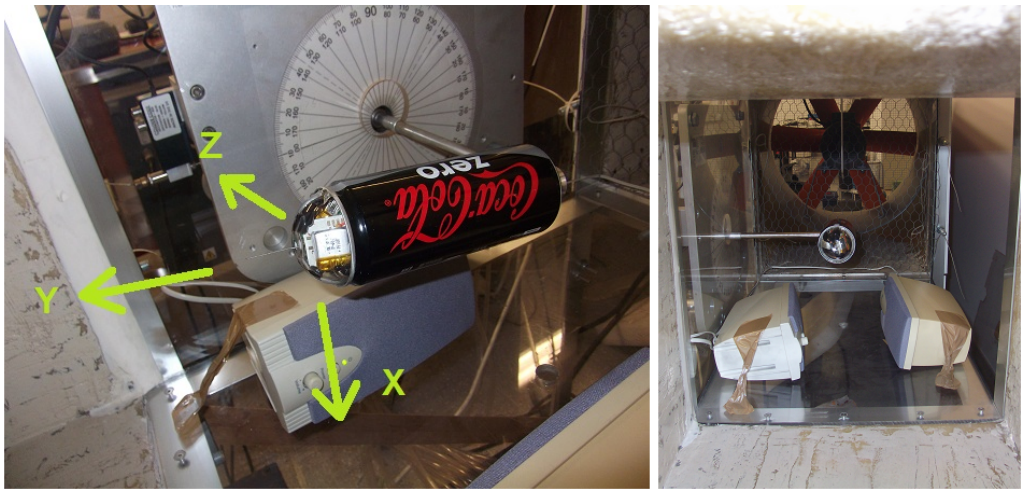


Figure 4.1: LIS331HH Accelerometer Breadboard and Wind Tunnel setup

The real Stage 2 were attached by an arm of steel of $20\,cm$ of length and $12\,mm$ of diameter. Interlink is based on two $M4$ bolts that provides enough rigidity to the mini-launcher. Protection measures were taken during the tests like ear protection and safe net. Before start the test, we should calibrate the wind tunnel because the area of the model generates a load for the propeller that can change the average speed flow provided by the manufacturer. The wind Tunnel manufacturer[4] defines that for a given motor frequency, it corresponds to a given wind speed. Figure 4.2 shows our calibrated equivalent average flow speed in $km/h$ units and $m/s$ units.

## 4.2. Basic Aerodynamic Parameters

A series of wind tunnel tests were done by changing the average wind speed (changing from $0\,m/s$ to $33\,m/s$) and angle of attack(varying from 0 degree to 10 degrees), in order to measure the Lift, the Drag and the Pitch moment. The results are given in annex A. From the measured data, the similar tendency for the aerodynamic parameters versus wind speed is found for different angles of attack.

[1] http://www.st.com/stonline/products/literature/ds/16366.pdf
[2] http://invensense.com/mems/gyro/documents/PS-ITG-3200-00-01.4.pdf
[3] http://cache.freescale.com/files/sensors/doc/data_sheet/MPL115A2.pdf?fpsp=1
[4] http://epsc.upc.edu/ca/fitxers/WT_UserManual1.pdf

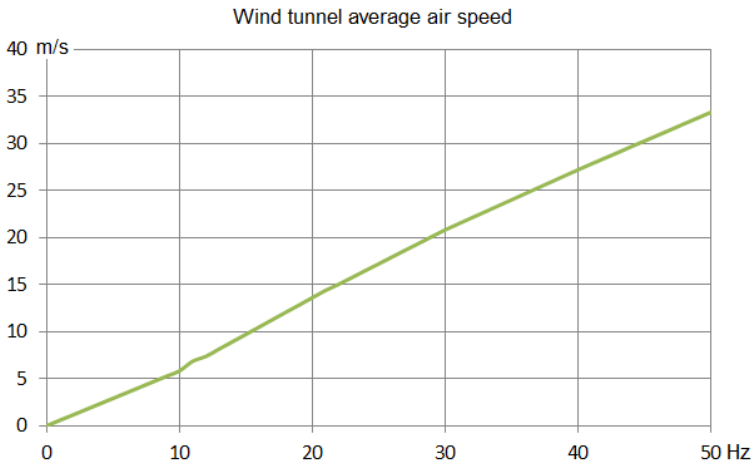


Figure 4.2: Relationship between Motor frequency and Wind tunnel air speed

## 4.3. Dynamic Test Results

The dynamic test is consist of sweep sine excited wind tunnel tests and operational vibration tests.

### 4.3.1. Test with Sweep Sine Excitation

Two sweep excited wind tunnel tests were done. One was to measure vibrations from the surrounding of the wind tunnel test chamber without wind and the other was to measure vibrations from the inside of the launcher with different wind speeds. *YouTube* video of this wind tunnel test can be seen here at http://www.youtube.com/watch?v=tmtI-cp0FUc Wikisat channel.

For the Frequency Response Function (FRF) the launcher is excited using two speakers as shown in figure 4.1 on right hand. Typical results are presented in figure 4.3. Unfortunately, we decided to use a range from $10\,Hz$ to $800\,Hz$ that are often used for commercial aircrafts. Later on it turned out that the smaller size of the launcher the higher frequency response it will be. And the lowest response frequency for mini-launcher may be in the range of $2,500\,Hz$ so the results showed in figure 4.3 are not useful for our case but it gives an important information about the wind tunnel and the low frequency response. This is due to the theory that these new kind of launchers are so small and frequency range should be from $2,000\,Hz$ that represents a length of less than $0.2\,m$, corresponding to the stage 2 structure length, until $7,000\,Hz$ that represents a length of less than $0.05\,m$ corresponding to the Stage 2 diameter.

In order to know the frequency response function for the launcher, firstly we need to know the wind tunnel frequency response and then we will subtract to the frequency response function of the system: Wind tunnel plus launcher. In future work, these series of excitation test should be done in a correct range. We do not appreciate any different frequency response produced by the launcher at the low frequency range that we have selected. Also, higher sampling rate should be selected from the on-board sensors. It is needed to

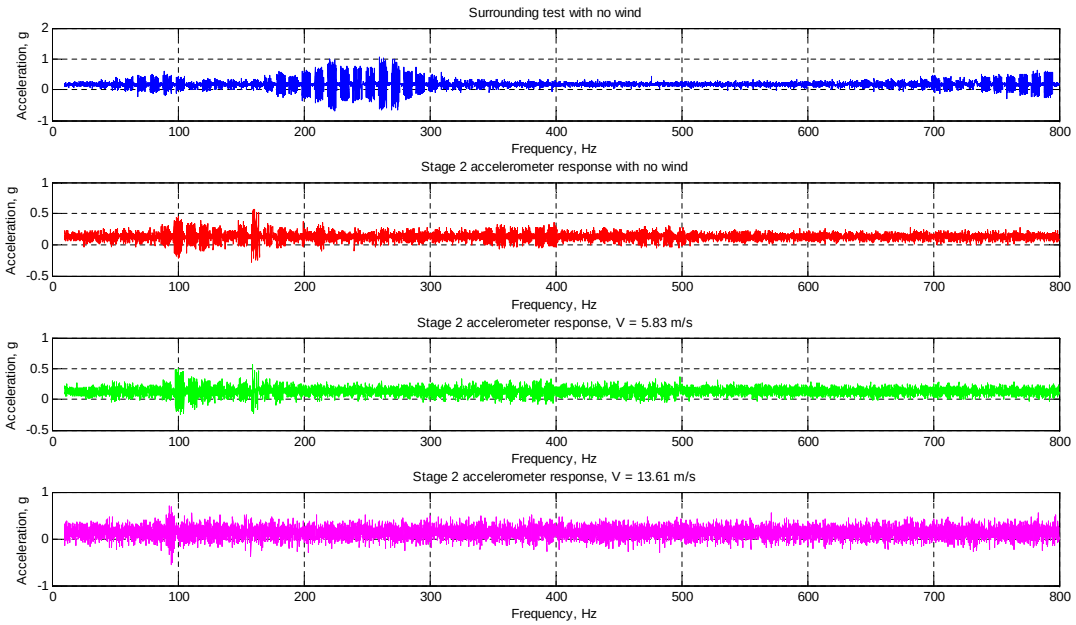


Figure 4.3: Responses with step sine excitation (frequency scope: $10\,Hz$ to $800\,Hz$)

say that the aforementioned series of test can not be repeated inside this master thesis due to the lack of time but they will be repeated very soon by the Wikisat team in order to complete the stage 2.

### 4.3.2. Test in Operational Condition

The operational modal test is done in terms of operating the launcher in different flight conditions, reading the accelerations, gyros, temperature and time stamp that we are receiving from the Stage 2 sensors. The flight conditions are changing the flight speed and the angle of attack. The time-domain responses are recorded and presented in annex B. These series of test has a lot of noise due to the flow and the wind tunnel motor. In order to reduce the noise we have studied the standard deviation of the vibration. We suspect that when the launcher has a large angle of attack, it will stall and then a vibration will be induced. For this reason we are interested in vibrations inside the plane XY that are AoA dependent. The aforementioned figure 4.1 has the axis distribution where the launcher arm turns around the axis Z normal to the plane XY. Figures 4.4, 4.5 and 4.6 provides some interesting results that will be discussed following.

The stall condition is detected between $20$ and $30$ degrees as expected. This stall condition generates a strong vertical oscillation because it is detected in the X axis but when the AoA increases beyond $60$ degrees, the oscillation turns horizontal and also is detected by the same axis that now is in vertical position. Opposite, the Y axis only detects some vibrations for high wind speeds. We can figured out that this kind of oscillation put to the limit the structure in the weakest direction. The result is the bending of the launcher and provoking a fold in the sheet of the can and turning unstable the launcher. We should mention that this operational mode study was done in subsonic conditions. In the real flight, we expect

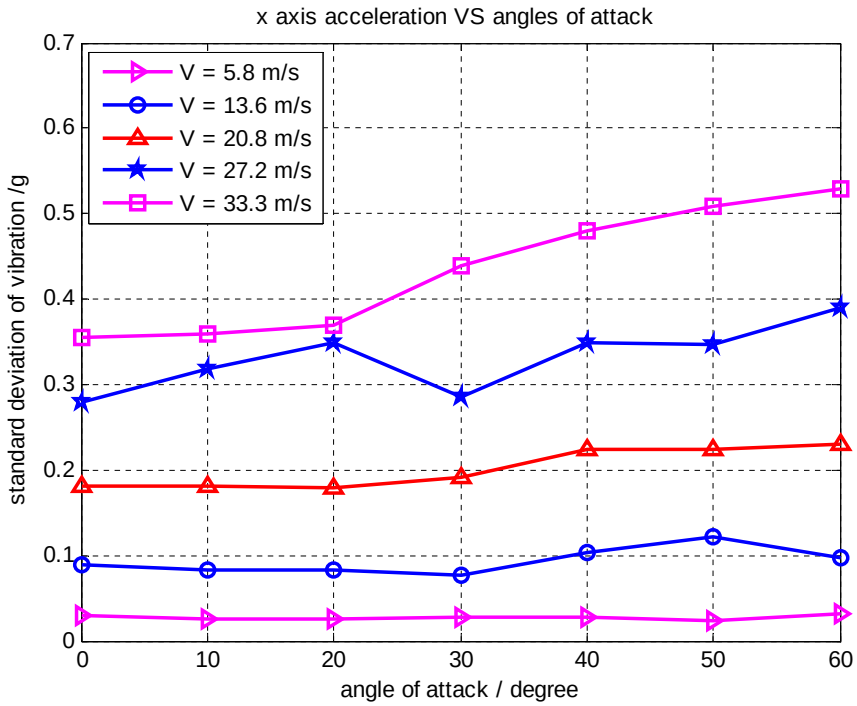


Figure 4.4: X axis vibration standard deviation vs angle of attack for different wind speeds

supersonic flight conditions and low density conditions. It is needed a different supersonic and hypersonic flight test in order to compare the operational modes with the ones we found in this tests.

Recommendations for the vector control subsystems are that it is better to keep the launcher below an angle of attach of $20$ degrees. Real simulations in terms of vector control done by Roberto Rodríguez [14] states an operative angle of $2$ degrees and the maximum allowed angle is set at $5$ degrees where it became unstable.

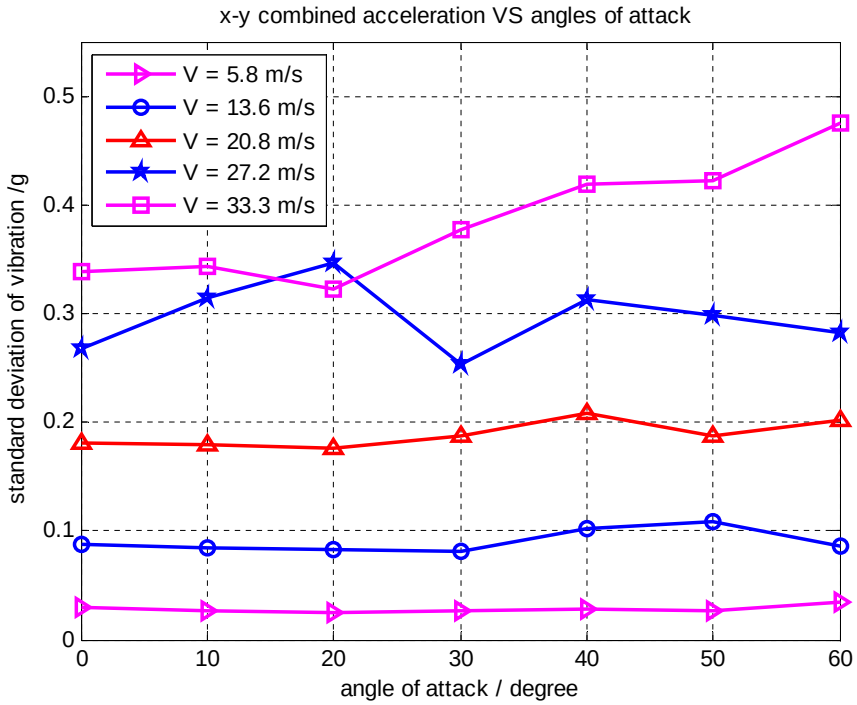


Figure 4.5: XY axes vibration standard deviation vs angle of attack for different wind speeds

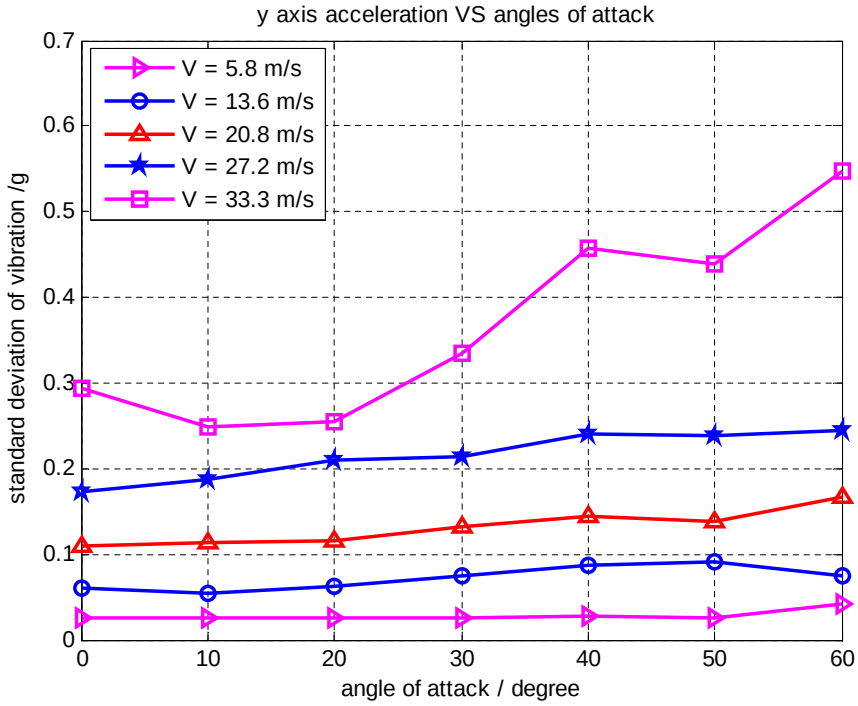


Figure 4.6: Y axis vibration standard deviation vs angle of attack for different wind speeds

# CHAPTER 5. REAL LAUNCH TEST

The main objective of this real test is twofold: one is to acquire knowledge about the vibrations in real flight and real environment and the other is to achieve supersonic speeds that were not possible to achieve in the wind tunnel that we used. There is a YouTube video of this real launch that can be seen here http://www.youtube.com/watch?v=264hK51WcXk in the Wikisat channel.

## 5.1. Preparation for the Launch

The initial flight was intended to be launched on ground at Sea level but inside the balloon like it will be in the real one. In normal conditions, the Wiki-launcher is ignited at $32\,km$ of altitude inside the balloon from a launching ramp. This launching ramp is connected to the balloon; inside there is an atmosphere of helium. The launcher ignition should provoke the burst and the launcher should pass trough the balloon. We decided to proceed that way to simplify the study, a real launch in near-space is costive and more complicated to manage. We putted helium inside the balloon as usual and the rest to simulate the burst condition is done with air. Unfortunately the air compressor that we wanted to use was weak and it takes few hours to have extra pressure inside. Additionally there was water condensation through the nozzle that react with the propellant. When we ignited the launcher, it failed. We decided to do a common launch without helium atmosphere in order to use a wick as a manual ignition method. The propellant was full of humidity and combustion was really bad but it flew. During the burnout a flame opened the launcher in order to deploy the parachute for recovery.

## 5.2. Launch Test Results

Figure 5.1 shows the time response of the flight. It is possible to see the vibrations due to the burnout and the impact with the ground. After the recovery, few hours later, the satellite still was alive and sending the telemetry. This fact validates once the robustness of the satellite against high accelerations, extreme temperatures and even fire conditions. The parachute deploy system failed because the strap was cut, the folding parachute offered to much tension to the cord. The flame burned the femto-satellite but it survived. The stability of the launcher was closer to neutral but trajectory, even was really slow, it was a parabolic flight. It is mandatory to use a full operative second stage in order to achieve higher speeds.

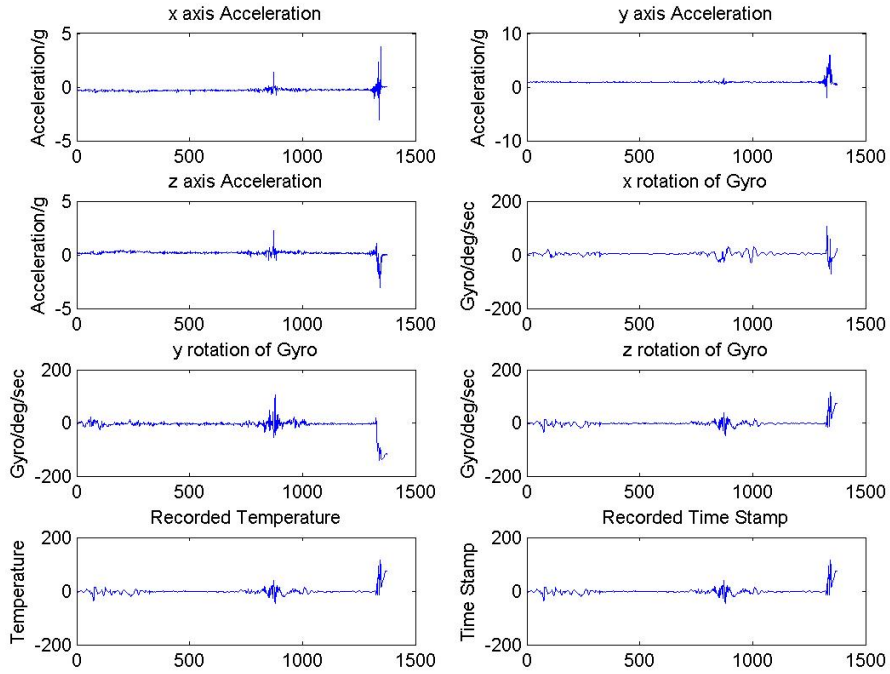


Figure 5.1: Time response of stage 2 during the real flight

# CONCLUSIONS

### 1. General conclusions

This thesis has explored the flutter prediction of a mini-launcher, utilizing a relatively new data-based flutter prediction approach, which is featured by the parameter-varying estimation (PVE) model. PVE predictor employs several modern techniques, such as PolyMAX modal extraction, Block-oriented identification, linear fraction transform (LFT) and structured singular analysis $\mu$-method, etc. The implementation is concluded into three main steps. And the effectiveness of the prediction approach is demonstrated by two typical application cases. Then as a new research, the application to a mini-launcher is explored and tested through wind tunnel and real launch tests.

### 2. Environmental impact

The flutter prediction framework is intended to improve the efficiency of flutter test, which is essential for the safety of flight vehicles, but also expensive and time-consuming. The PVE method studied in this thesis proved to be effective with a small amount of flight waypoints, which may lead to a drastically reduction of waste production and energy consumption. And some equipments, like sensors for the tests are recycled. Since the Wiki-launcher is of a mini size, the environment impact is also very small.

### 3. Future work

This is just a beginning for the exploration of flutter analysis and prediction concerned with mini-launcher. There remain many possible improvements for further investigation. For instance, due to the small sizes, a good net of sensors like accelerometers or others should be better designed. It means not only to be smaller to reduce its influences, but also to be most efficient for the DAQ of the prediction work. The impact of internal flow in the mini-launcher may be studied by more tests to find the most dangerous scenario during the whole launch, and the flutter boundary could be predicted effectively and rapidly, even on-line, thus some modification can be made to avoid a potential failure due to flutter effect.

# GLOSSARY

**AoA.** Angle of Attack

**APCP.** Ammonium Perchlorate Composite Propellant

**CPU.** Central Processing Unit

**DAQ.** Data Acquisition

**DOF.** Degree-of-Freedom

**EMA.** Experimental Modal Analysis

**FRF.** Frequency Response Function

**GND.** Ground

**GUI.** Graphical User Interface

**HGA.** High Gain Antenna

**LEO.** Low Earth Orbit

**LFT.** Linear Fraction Transform

**MCU.** Main Control Unit

**MEMS.** Micro-Electro-Mechanical Systems

$\mu$**.** Structured Singular Value

$\Delta$**.** Uncertainty of Model

**0MA.** Operational Modal Analysis

**PolyMAX.** Poly-reference Weighted Least Squares Complex Frequency-domain estimator (p-LSCF)

**PVC.** Polyvinyl Chloride

**PVE.** Parameter Varying Estimation

**SCL.** $I^2C$(Inter-Integrated Circuit) Serial Clock

**SDA.** $I^2C$ Serial Data

**SNR.** Singal-to-Noise Ratio

$V_{cc}$**.** $I^2C$ Positive Power Supply Pin

**Z-W.** Zimmerman-Weissenburger (flutter margin method)

# BIBLIOGRAPHY

[1] R. Lind, “Flight-Test Evaluation of Flutter Prediction Methods”, Journal of Aircraft, vol.40(5), 2003

[2] M.W. Kehoe, “A Historical Overview of Flight Flutter Testing”, NASA TM-4720, 1995

[3] N.H. Zimmerman, J.T. Weissenburger, “Prediction of Flutter Onset Speed Based on Flight Testing at Subcritical Speeds”, Journal of Aircraft, vol.1(4), 1964

[4] R. Lind, M. Brenner, “Flutterometer: An On-Line Tool to Predict Robust Flutter Margins”, Journal of Aircraft, vol.37(6), 2000

[5] R. Lind, “Match-Point Solutions for Robust Flutter Analysis”, Journal of Aircraft, vol.39(1), 2002

[6] D.H. Baldelli, J. Zeng., R. Lind, et al., “Flutter-Prediction Tool for Flight-Test-Based Aeroelastic Parameter-Varying Models”, Journal of Guidance, Control, and Dynamics, 2009

[7] R. Lind, M.Brenner, “Robust Aeroservoelastic Stability Analysis. Flight Test Applications”,Springer-Verlag London Limited, 1999

[8] D.H. Baldelli, R. Lind, M. Brenner, “Control-Oriented Flutter/Limit-Cycle-Oscillation Prediction Framework, vol.31(6), 2008

[9] D. Barnhart, et al., “System-on-a-Chip Design of Self-Powered Wireless Sensor Nodes for Hostile Environments”, 2007 IEEE Aerospace Conference, Montana (2007)

[10] R. Jove, et al., “Technical constrains for a low cost femto-satellite launcher”, 49th AIAA Aerospace Sciences Meeting. (January 2011)

[11] Bonet, L., “High altitude balloon mission design and implementation for a mini-launcher”, Bachelor work, upcommons, 2011

[12] Bardolet, E., “Study of a low cost inertial platform for a femto-satellite deployed by a mini-launcher”, Bachelor work, upcommons, 2010

[13] Kravchenko, V., “Design and implementation of a femto-satellite technology demonstrator”, Master thesis, upcommons, 2011

[14] Rodriguez, R., “Study of a nozzle vector control for a low cost mini-launcher”, Master thesis, upcommons, 2011

[15] Dewey H. Hodge, G. Alvin Pierce, “Introduction toi Structural Dynamics and Aeroelasticity”, Cambridge University Press, 2002

[16] ZAERO, Theoretical Manual, Ver.8.2, ZONA Technology Inc., Scottsdale, AZ, Mar. 2008.

[17] D.J.Johns, “A Survey on Panel Flutter”, 21st Meeting of the AGARD Structures and Materials Panel, Nancy, France, November 1965

[18] B. Cauberghe, “Applied Frequency-domain System Identification in the Field of Experimental and Operational Modal Analysis” PhD These, 2004

[19] B. Cauberghe, P. Guillaume, P. Verboven, et al., “On the influence of the parameter constraint on the stability of the poles and the discrimination capabilities of the stabilisation diagrams”, Mechanical System and Signal Processing, 2005

[20] J.C. Gomez, E. Baeyens, “Identification of Block-oriented Nonlinear Systems Using Orthonormal Bases” Journal of Process Control, vol.14, pp.685-697, 2004

[21] D.H. Baldelli, R. Lind, M. Brenner, “Nonlinear Aeroelastic/Aeroservoelastic Modeling by Block-Oriented Identification”, vol.28(5), 2005

[22] J. Zeng, D.H. Baldelli, M. Brenner, “Identification of Nonlinear Hammerstein System Using Orthonormal Bases: Application to Nonlinear Aeroelastic/Aeroservoelastic System”, AIAA Atmospheric Flight Mechanics Conference and Exhibit, 2007

[23] B. Ninness, F. Gustafsson, “A Unifying Construction of Orthonormal Bases for System Identification”, Technical Report, 1994

[24] Jeonghwan Ko, Andrew J.Kurdila, Thomas W.Strganac “Nonlinear Control of a Prototypical Wing Section with Torsional Nonlinearity” Journal of Guidance, Control, and Dynamics, Vol.20, No.6, November-December 1997

# APPENDIX A. TEST RESULTS OF THE LIFT, DRAG AND PITCH MOMENT

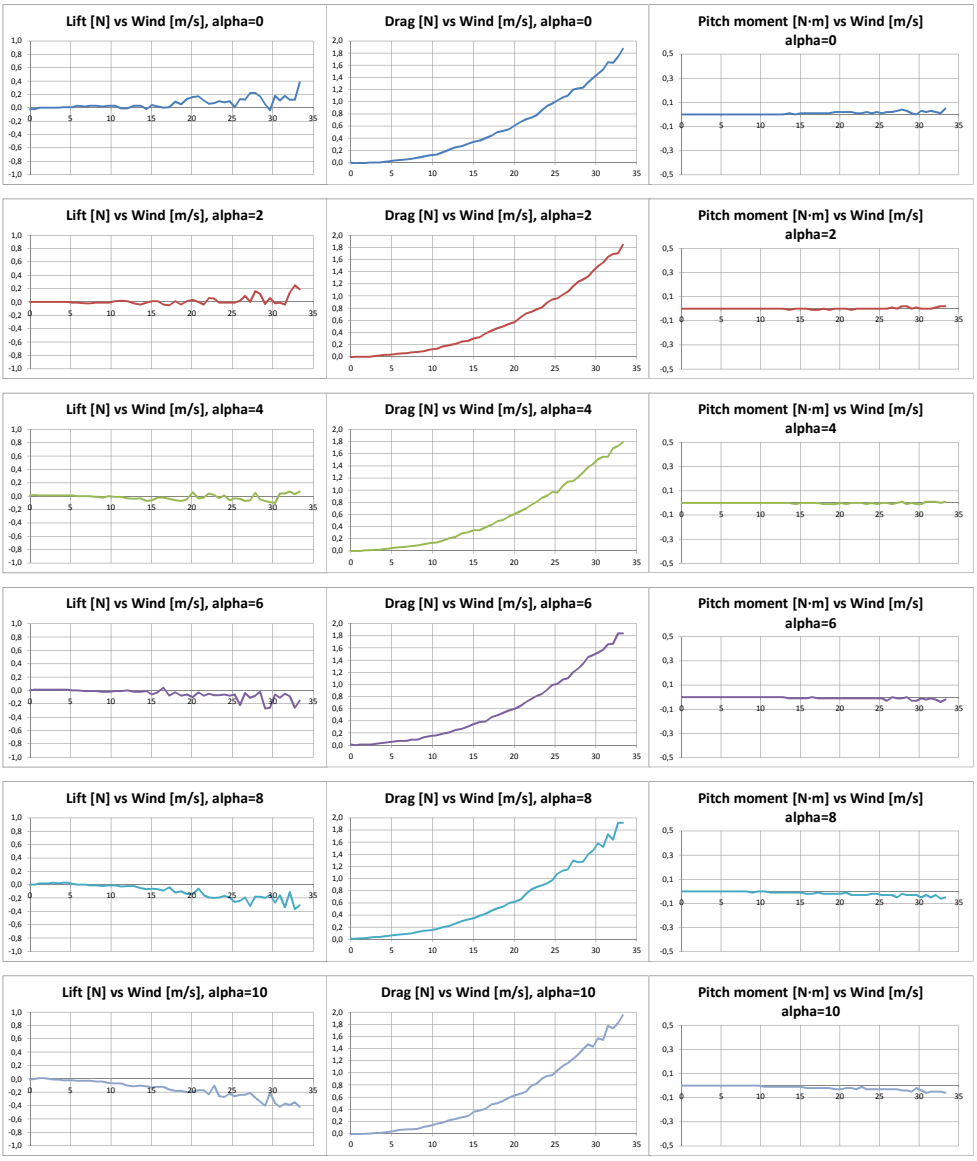


**Stage 2. Length = 145 mm, Diameter = 55 mm (Angle of attack in degrees)**

Figure A.1: Measured Lift, Drag and Pitch moment varied with wind speed and angle of attack

# APPENDIX B. TIME-DOMAIN RESPONSE

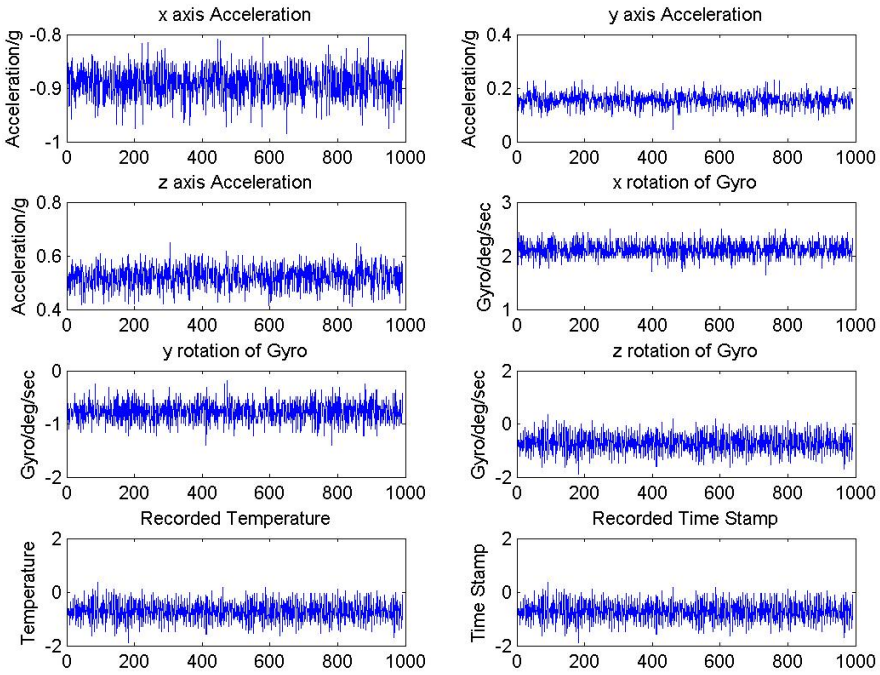


Figure B.1: Time response of Stage 2 for the wind at $5.8 m/s$ and AoA of $0$ degrees

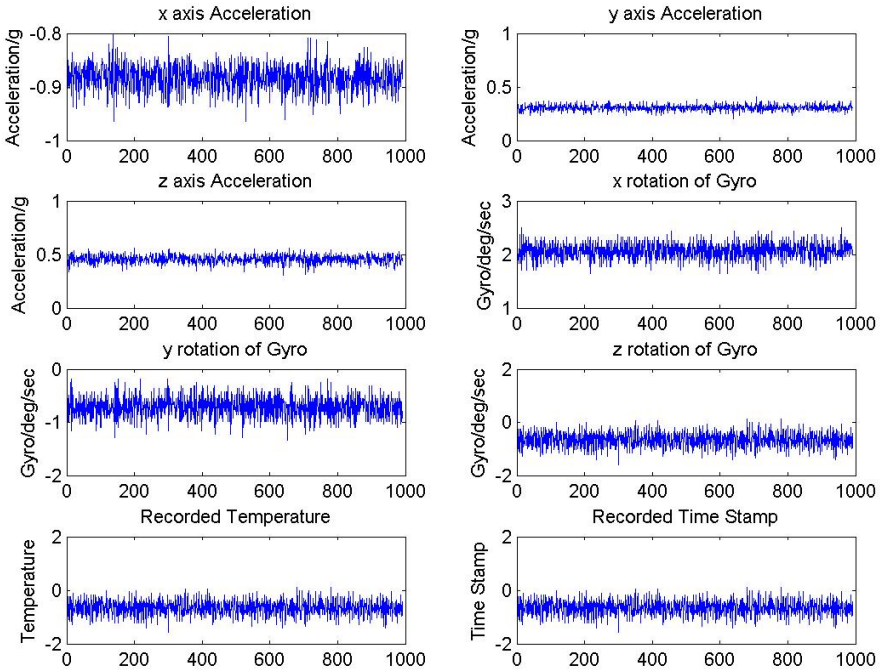


Figure B.2: Time response of Stage 2 for the wind at $5.8 m/s$ and AoA of $10$ degrees

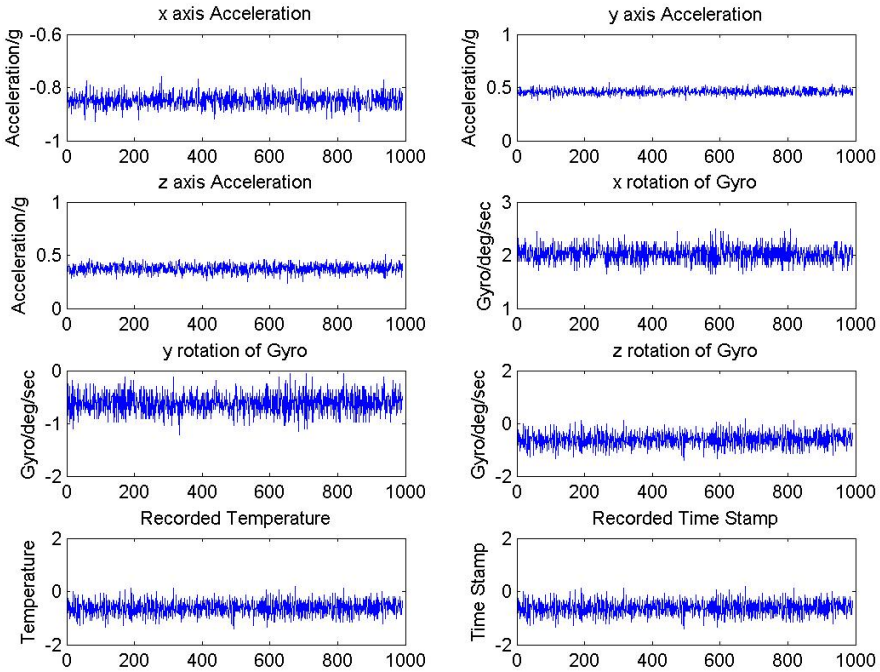


Figure B.3: Time response of Stage 2 for the wind at $5.8 m/s$ and AoA of $20$ degrees

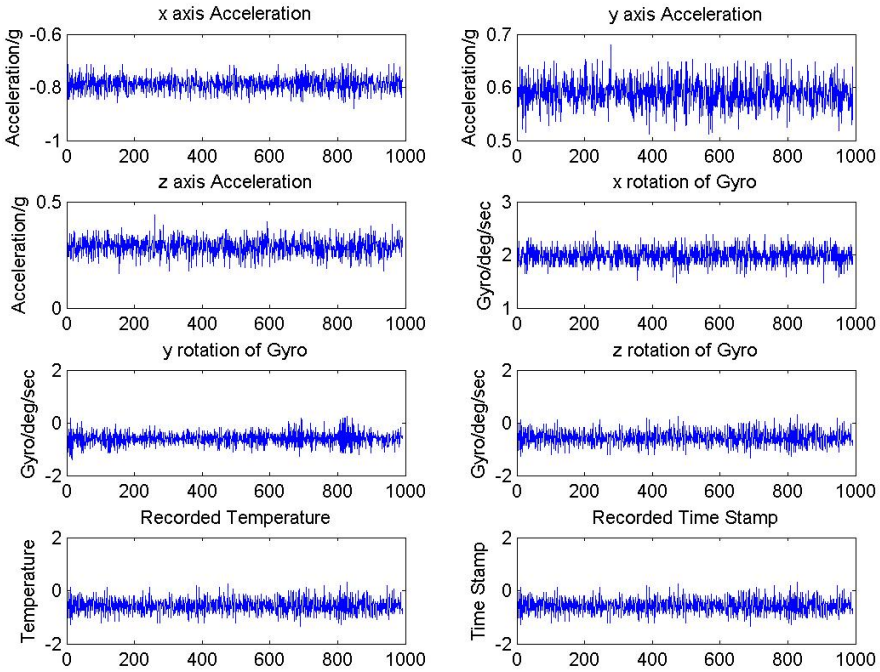


Figure B.4: Time response of Stage 2 for the wind at $5.8 m/s$ and AoA of $30$ degrees

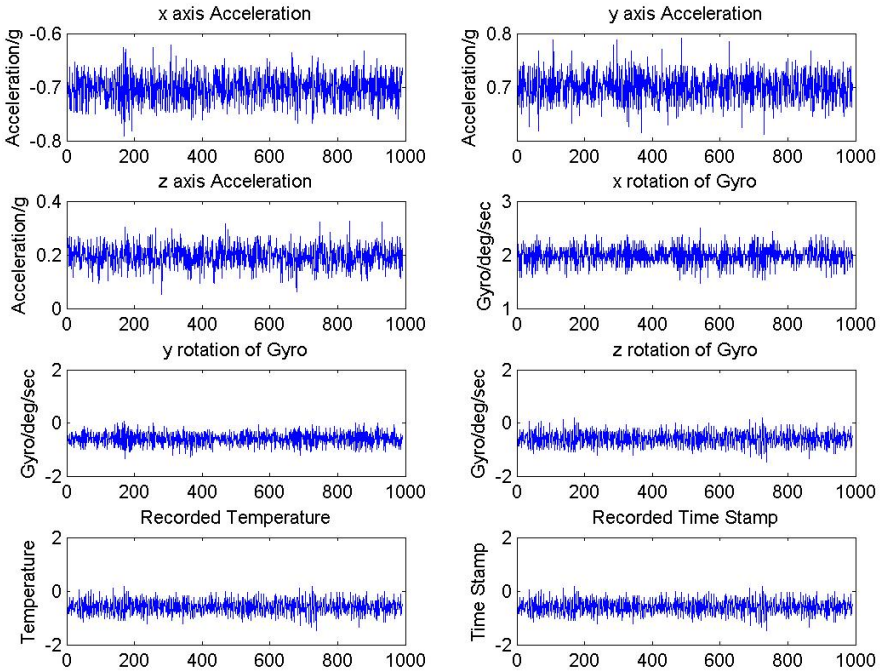


Figure B.5: Time response of Stage 2 for the wind at $5.8 m/s$ and AoA of $40$ degrees

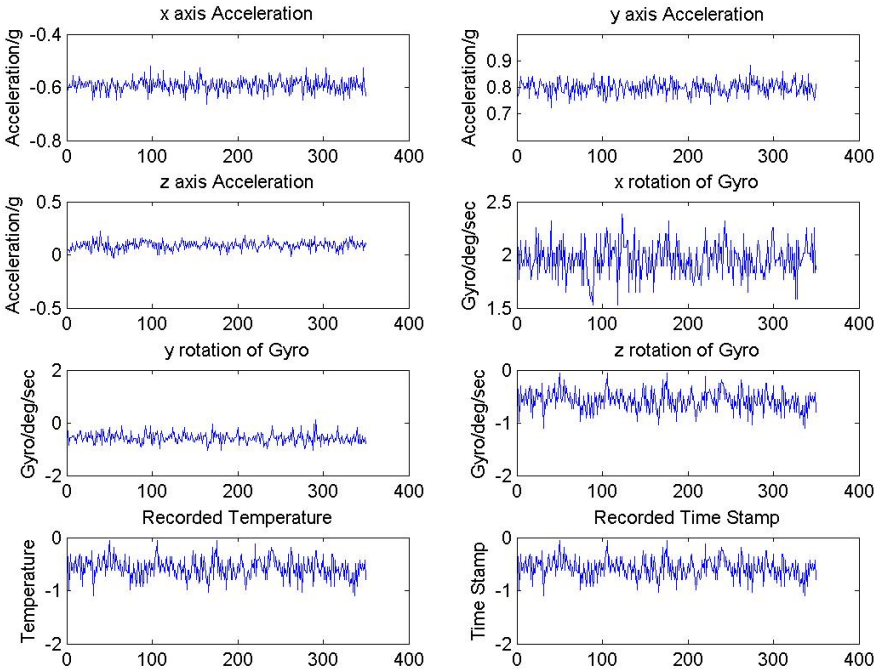


Figure B.6: Time response of Stage 2 for the wind at $5.8 m/s$ and AoA of $50$ degrees

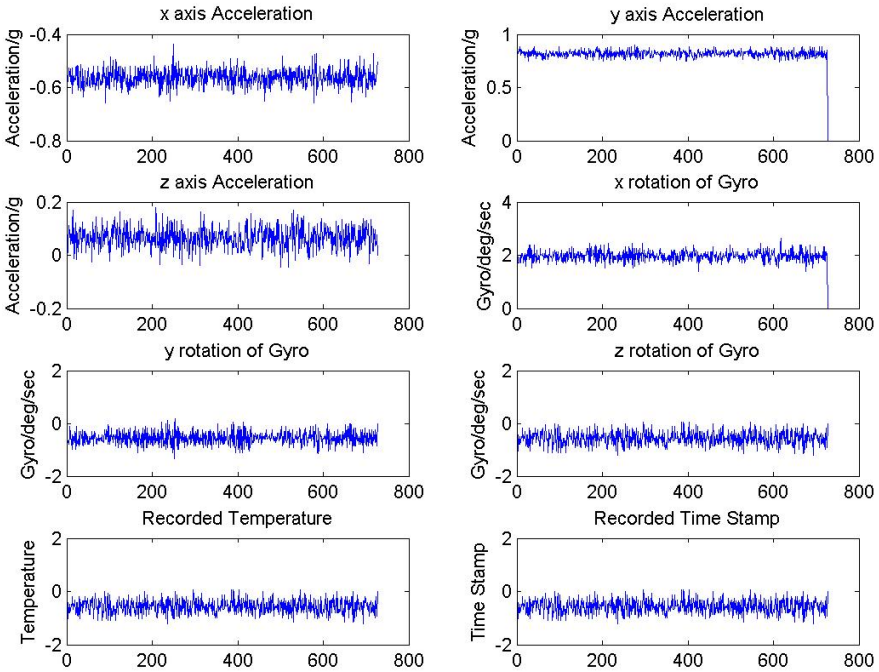


Figure B.7: Time response of Stage 2 for the wind at $5.8 m/s$ and AoA of $60$ degrees

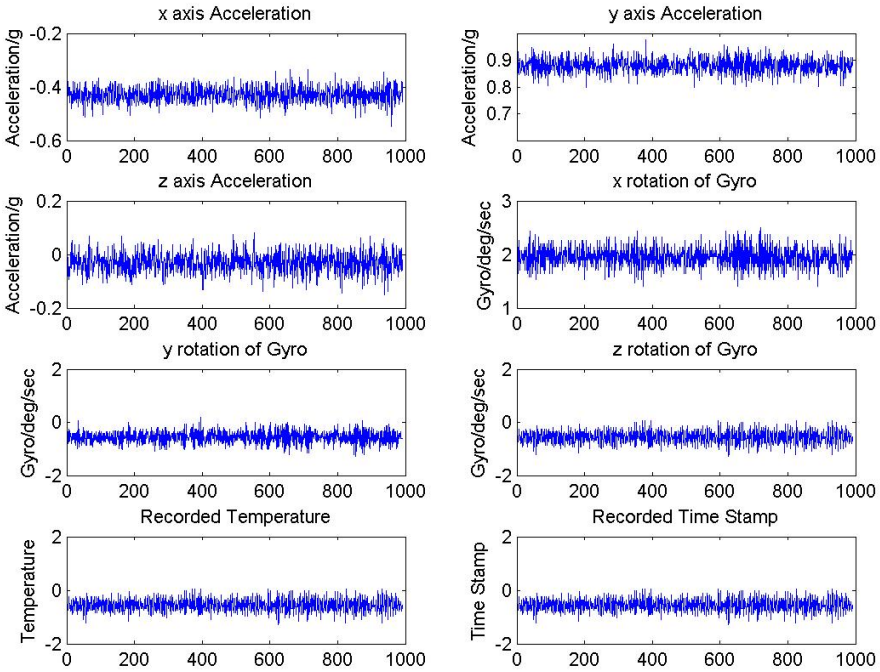


Figure B.8: Time response of Stage 2 for the wind at $5.8 m/s$ and AoA of $70$ degrees

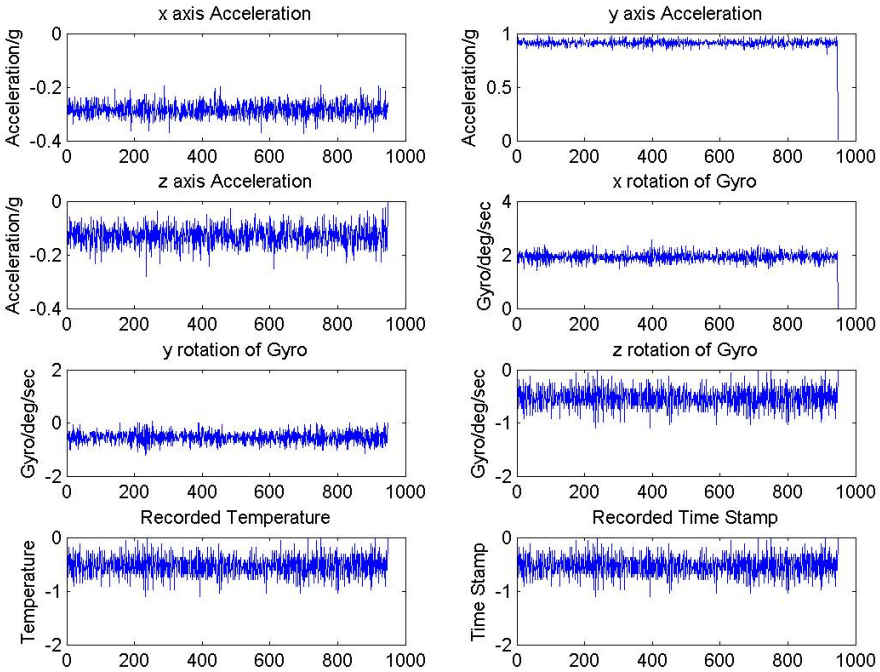


Figure B.9: Time response of Stage 2 for the wind at $5.8 m/s$ and AoA of $80$ degrees

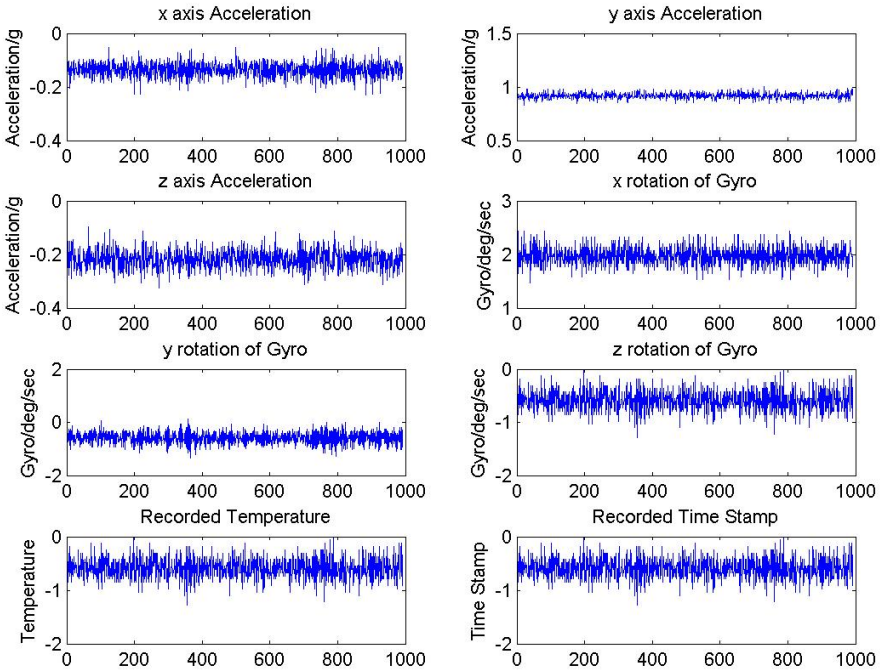


Figure B.10: Time response of Stage 2 for the wind at $5.8 m/s$ and AoA of $90$ degrees

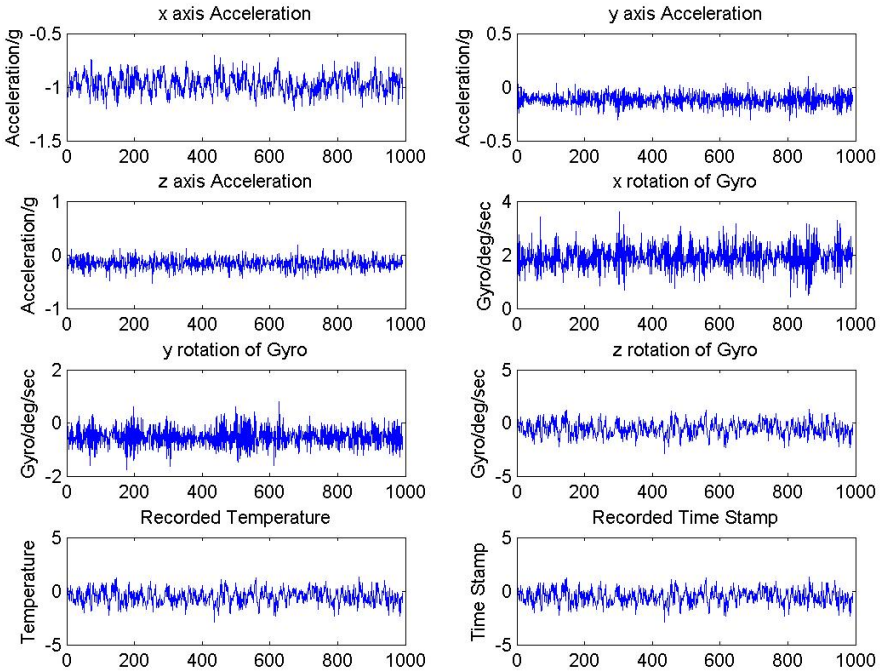


Figure B.11: Time response of Stage 2 for the wind at $13.6 m/s$ and AoA of $0$ degrees

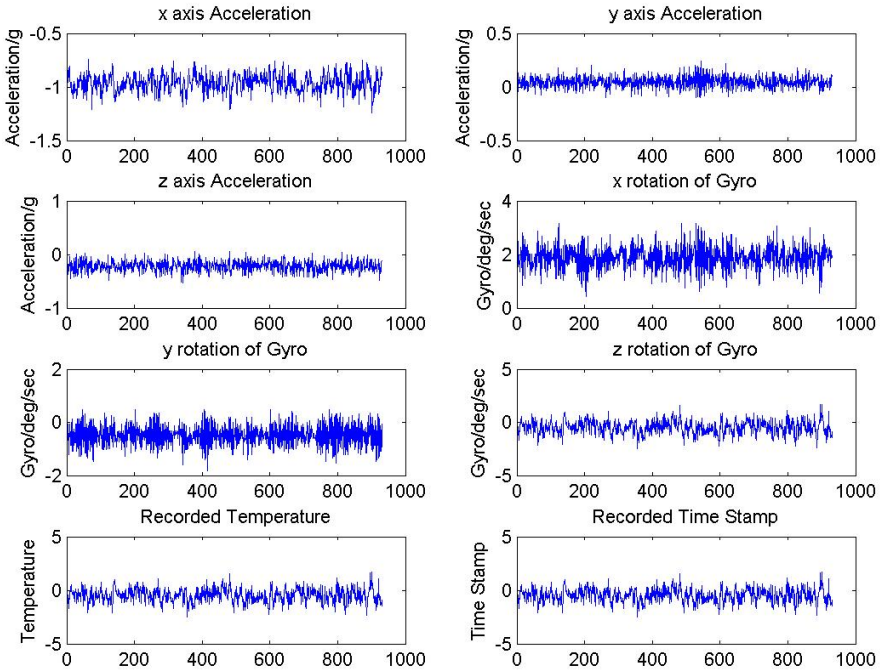


Figure B.12: Time response of Stage 2 for the wind at $13.6 m/s$ and AoA of $10$ degrees

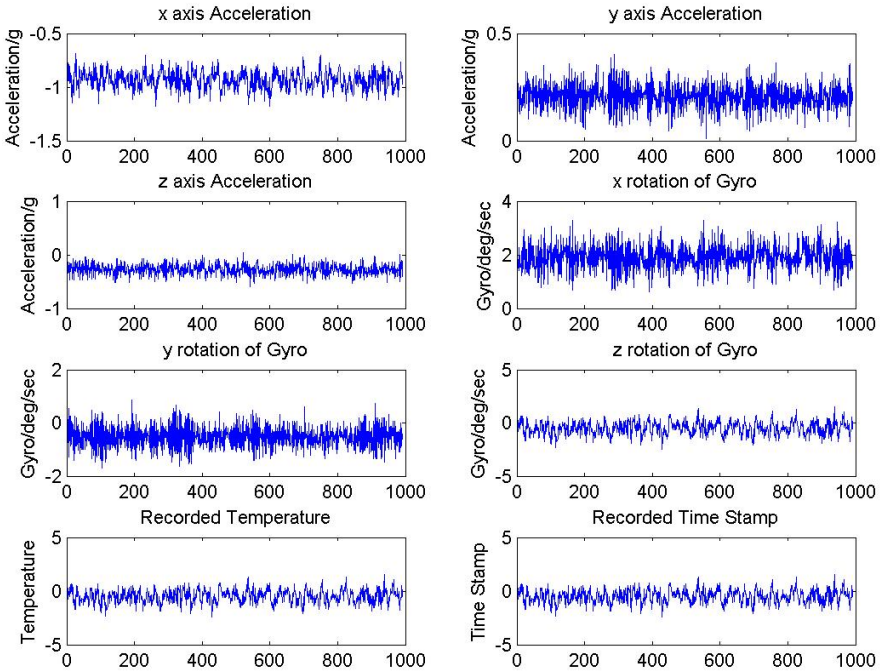


Figure B.13: Time response of Stage 2 for the wind at $13.6 m/s$ and AoA of $20$ degrees

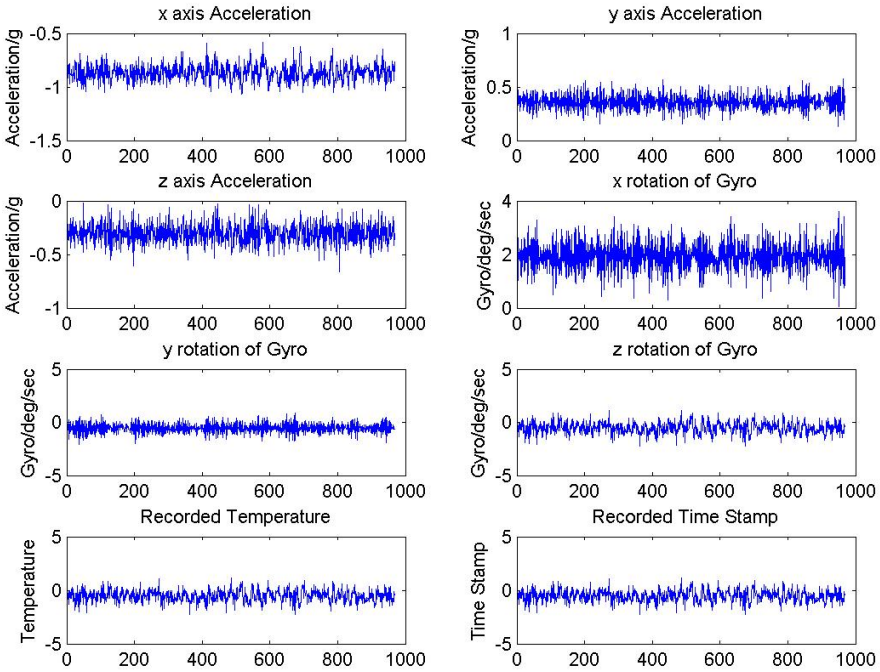


Figure B.14: Time response of Stage 2 for the wind at $13.6 m/s$ and AoA of $30$ degrees

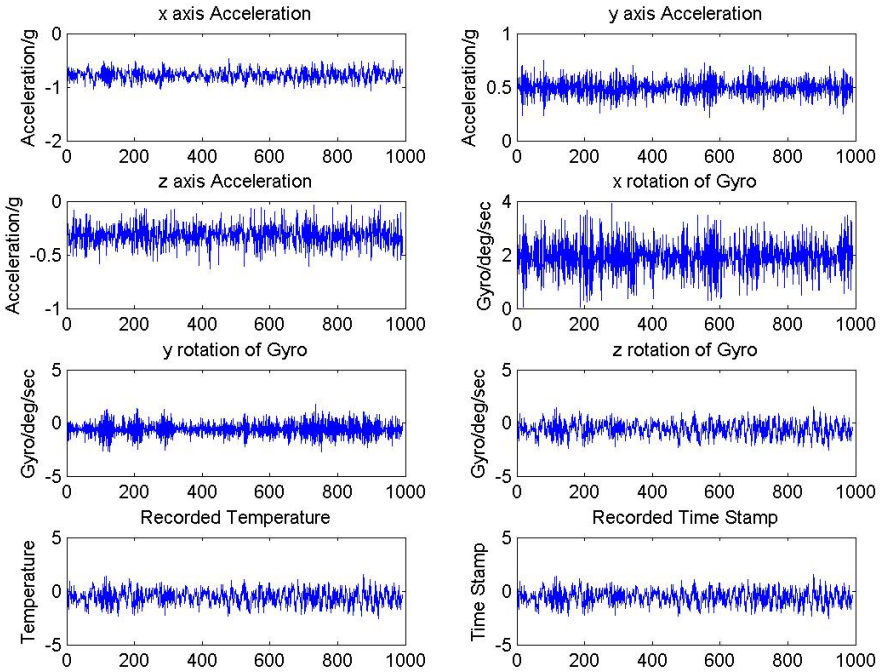


Figure B.15: Time response of Stage 2 for the wind at $13.6 m/s$ and AoA of $40$ degrees

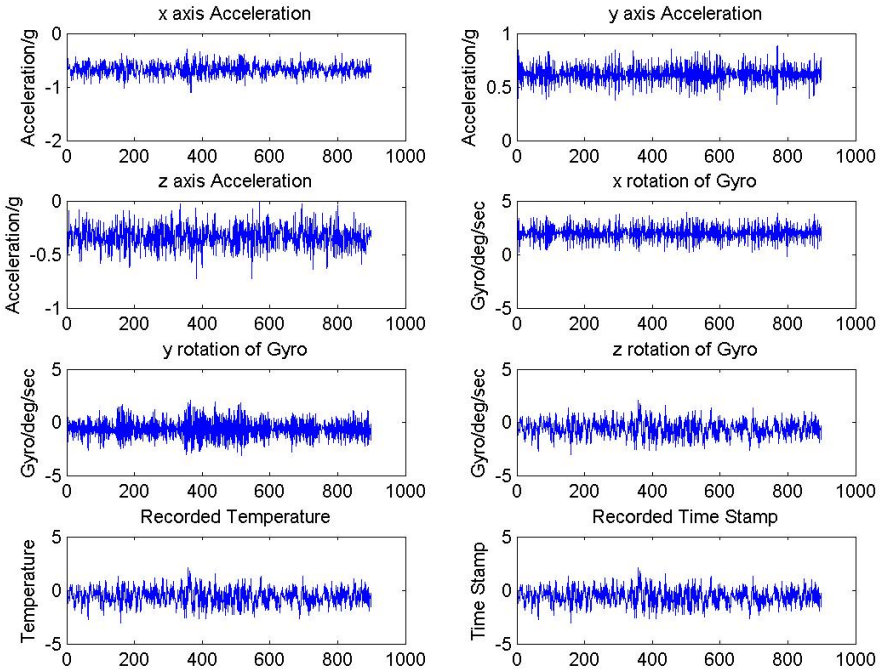


Figure B.16: Time response of Stage 2 for the wind at $13.6 m/s$ and AoA of $50$ degrees

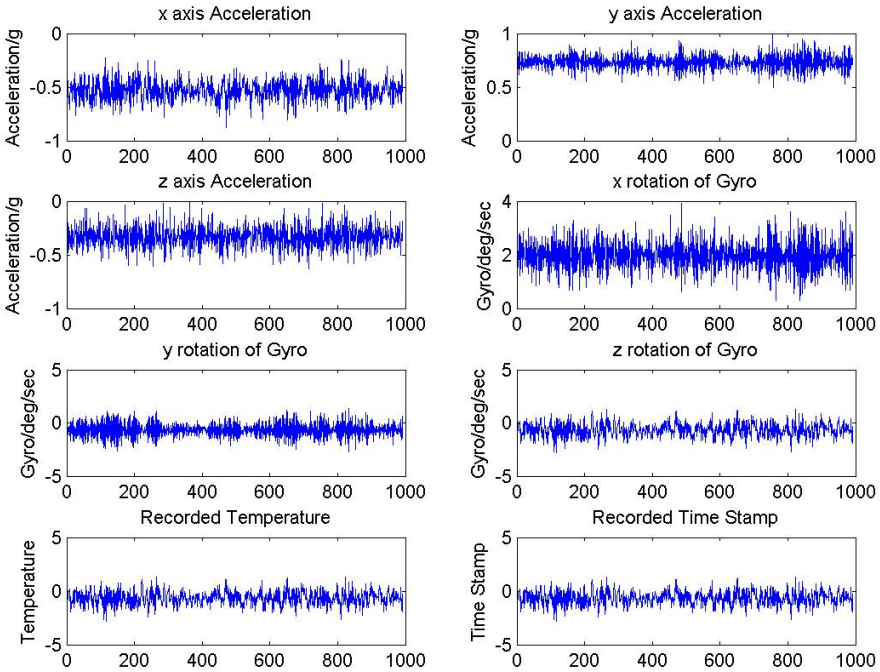


Figure B.17: Time response of Stage 2 for the wind at $13.6 m/s$ and AoA of $60$ degrees

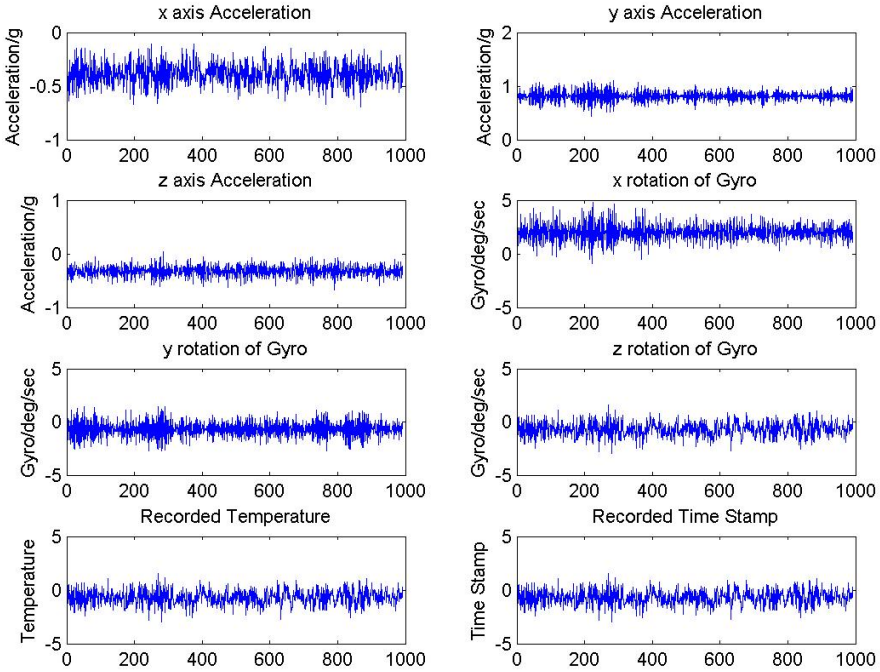


Figure B.18: Time response of Stage 2 for the wind at $13.6 m/s$ and AoA of $70$ degrees